
Masters Theses

Student Theses and Dissertations

Spring 1987

The effect of excess lead oxide on the sintering characteristics and dielectric properties of lead magnesium niobate ceramics

Dyllan Jye-Lun Hong

Follow this and additional works at: https://scholarsmine.mst.edu/masters_theses



Part of the [Ceramic Materials Commons](#)

Department:

Recommended Citation

Hong, Dyllan Jye-Lun, "The effect of excess lead oxide on the sintering characteristics and dielectric properties of lead magnesium niobate ceramics" (1987). *Masters Theses*. 460.
https://scholarsmine.mst.edu/masters_theses/460

This thesis is brought to you by Scholars' Mine, a service of the Missouri S&T Library and Learning Resources. This work is protected by U. S. Copyright Law. Unauthorized use including reproduction for redistribution requires the permission of the copyright holder. For more information, please contact scholarsmine@mst.edu.

THE EFFECT OF EXCESS LEAD OXIDE ON THE SINTERING
CHARACTERISTICS AND DIELECTRIC PROPERTIES
OF LEAD MAGNESIUM NIOBATE CERAMICS

BY

DYLLAN JYE-LUN HONG, 1961-

A THESIS

Presented to the Faculty of the Graduate School of the

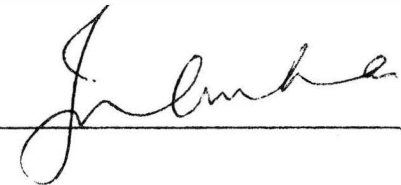
UNIVERSITY OF MISSOURI-ROLLA

In Partial Fulfillment of the Requirements for the Degree

MASTER OF SCIENCE IN CERAMIC ENGINEERING

1987

Approved by

 (Advisor) 


ABSTRACT

The effect of lead oxide additions on sintering characteristics and dielectric properties of ferroelectric $\text{Pb}_3\text{MgNb}_2\text{O}_9$ based capacitors was studied. The basic dielectric compositions were formed by solid state reaction. Densification was studied as a function of PbO content over the temperature range 900°C to 1000°C for sintering times one to six hours depending on the amount of additive, and the sintering temperature.

Weight loss, density and shrinkage measurements of each composition were made in order to relate the effects of the excess PbO additions on the densification. The dielectric and electrical properties were then correlated to the microstructure and density.

The compositions sintered at low temperatures were densified by the formation of a liquid phase during sintering. However, an increase of the amount of liquid phase does not necessarily yield optimum dielectric properties. A proper control of the sintering temperature, time and the amount of excess PbO is required for optimization of the dielectric properties.

ACKNOWLEDGEMENT

The author expresses his sincere appreciation to Dr. Harlan Anderson for his suggestion of the subject of this study and to Dr. Jyoti Guha for his advice. The author also wishes to thank Daniel Beck for his assistance in operating the equipment and with the computer programming used in this study.

TABLE OF CONTENTS

	PAGE
ABSTRACT.....	ii
ACKNOWLEDGEMENT.....	iii
LIST OF ILLUSTRATIONS.....	vi
I. INTRODUCTION.....	1
II. REVIEW OF LITERATURE.....	6
III. EXPERIMENTAL PROCEDURE.....	10
A. STARTING MATERIALS AND PREPARATION.....	10
B. CAPACITOR PREPARATION AND SINTERING.....	11
C. PHYSICAL PROPERTY MEASUREMENTS.....	12
D. DIELECTRIC AND ELECTRICAL PROPERTY MEASUREMENTS.....	13
E. X-RAY DIFFRACTION ANALYSIS.....	14
F. MICROSTRUCTURE DEVELOPMENT.....	14
IV. RESULTS AND DISCUSSION.....	15
A. REACTIONS AND PHASE EQUILIBRIA.....	15
B. WEIGHT LOSS.....	17
C. SINTERING CHARACTERISTICS.....	22
D. MICROSTRUCTURES.....	29
E. DIELECTRIC AND ELECTRICAL PROPERTIES.....	36
V. CONCLUSION.....	48
BIBLIOGRAPHY.....	49
VITA.....	55
APPENDICES.....	56
A. CALCULATION FOR THEORETICAL DENSITY.....	56

TABLE OF CONTENTS (Continued)

	PAGE
B. SAMPLE BULK DENSITY, SHRINKAGE AND WEIGHT LOSS.....	58
C. MAXIMUM DIELECTRIC CONSTANT, CURIE TEMPERATURE, DISSIPATION FACTOR AND RESISTIVITY AT T_c	61

LIST OF ILLUSTRATIONS

FIGURE	PAGE
1(A). X-Ray Diffraction Pattern Resulting from the Direct Reaction of $\text{PbO-MgO-Nb}_2\text{O}_5$ at 800°C	16
1(B). X-Ray Diffraction Pattern Resulting From the Reaction of PbO and MgNb_2O_6 at 800°C	16
1(C). X-Ray Diffraction Pattern Resulting From the Reaction of PbO and MgNb_2O_6 at 800°C with Excess MgO	16
2. Weight Loss vs. Sintering Time for $\text{P}_3\text{MN-PT}$ with Excess PbO Sintered at 900°C	18
3. Weight Loss vs. Sintering Time for $\text{P}_3\text{MN-PT}$ with Excess PbO Sintered at 950°C	20
4. Weight Loss vs. Sintering Time for $\text{P}_3\text{MN-PT}$ with Excess PbO Sintered at 1000°C	21
5. Density vs. Weight Loss for $\text{P}_3\text{MN-PT}$ with Excess PbO Sintered at 900°C	23
6. Density vs. Weight Loss for $\text{P}_3\text{MN-PT}$ with Excess PbO Sintered at 950°C	24
7. Density vs. Weight Loss for $\text{P}_3\text{MN-PT}$ with Excess PbO Sintered at 1000°C	25
8. Density and Weight Loss vs. Sintering Temperature for $\text{P}_3\text{MN-PT}$ with Excess PbO Sintered for 3h.....	27
9. Density and Weight Loss vs. Sintering Temperature for $\text{P}_3\text{MN-PT}$ with Excess PbO Sintered for 5h.....	28

LIST OF ILLUSTRATIONS (Continued)

	PAGE
10. SEM Photomicrograph of a Fracture Surface of P ₃ MN-PT with 2.5 m% Excess PbO Sintered for 1 h at 950°C (PbO Loss: 1.47 m%).....	30
11. SEM Photomicrograph of a Sintered Surface of P ₃ MN-PT with 2.5 m% Excess PbO Sintered for 1 h at 950°C (PbO Loss: 1.47 m%).....	30
12. SEM Photomicrograph of a Sintered Surface of P ₃ MN-PT with 2.5 m% Excess PbO Sintered for 3 h at 950°C (PbO Loss: 2.13 m%).....	31
13. SEM Photomicrograph of a Fracture Surface of P ₃ MN-PT with 2.5 m% Excess PbO Sintered for 3 h at 950°C (PbO Loss: 2.13 m%).....	31
14. SEM Photomicrograph of a Fracture Surface of P ₃ MN-PT with 2.5 m% Excess PbO Sintered for 3 h at 950°C (PbO Loss: 2.13 m%).....	32
15. SEM Photomicrograph of a Sintered Surface of P ₃ MN-PT with 2.5 m% Excess PbO Sintered for 5 h at 950°C (PbO Loss: 2.63 m%).....	32
16. SEM Photomicrograph of a Fracture Surface of P ₃ MN-PT with 2.5 m% Excess PbO Sintered for 5 h at 950°C (PbO Loss: 2.63 m%).....	34
17. SEM Photomicrograph of a Fracture Surface of P ₃ MN-PT with 3.3 m% Excess PbO Sintered for 2 h at 950°C (MgO ←).....	34

LIST OF ILLUSTRATIONS (Continued)

	PAGE
18. SEM Photomicrograph of a Fracture Surface of P_3MN -PT with 3.3 m% Excess PbO Sintered for 1 h at 1000°C (PbO Loss: 2.6 m%).....	35
19. SEM Photomicrograph of a Polished and Etched Section of P_3MN -PT with 3.3 m% Excess PbO Sintered for 1 hour at 1000°C (PbO Loss: 2.6 m%)....	35
20. SEM Photomicrograph of a Polished and Etched Section of P_3MN -PT with 3.3 m% Excess PbO Sintered for 2 hours at 1000°C (PbO Loss: 3.6 m%)...	37
21. SEM Photomicrograph of a Polished and Etched Section of P_3MN -PT with 3.3 m% Excess PbO Sintered for 3 hours at 1000°C (PbO Loss: 4.75 m%)..	37
22. Dielectric Constant vs. Temperature for P_3MN -PT with 3.3 m% Excess PbO Sintered for 3 h at 900°C....	38
23. Dissipation Factor vs. Temperature for P_3MN -PT with 3.3 m% Excess PbO Sintered for 3 h at 900°C....	39
24. Dielectric Constant vs. Temperature for P_3MN -PT with 3.3 m% Excess PbO Sintered for 3 h at 950°C....	40
25. Dissipation Factor vs. Temperature for P_3MN -PT with 3.3 m% Excess PbO Sintered for 3 h at 950°C....	41
26. Dielectric Constant vs. Temperature for P_3MN -PT with 3.3 m% Excess PbO Sintered for 3h at 1000°C....	42
27. Dissipation Factor vs. Temperature for P_3MN -PT with 3.3 m% Excess PbO Sintered for 3h at 1000°C....	43

LIST OF ILLUSTRATIONS (Continued)

PAGE

28.	Maximum Dielectric Constant at 1 KHZ vs. Sintering Temperature for P_3 MN-PT with Excess PbO Sintered for 3h.....	45
29.	Maximum Dielectric Constant at 1 KHZ vs. Sintering Temperature for P_3 MN-PT with Excess PbO Sintered for 5h.....	46

I. INTRODUCTION

Lead magnesium niobate ($\text{Pb}_3\text{MgNb}_2\text{O}_9$) belongs to a group of complex compounds known as ferroelectric relaxors¹. Due to its outstanding dielectric and electrostrictive properties this compound has been extensively studied since it was first reported in the late 1950's. The purpose of this study was to investigate the dielectric properties and low temperature densification of $\text{Pb}_3\text{MgNb}_2\text{O}_9$ - PbTiO_3 (hereafter designated as P_3MN and PT , respectively) based compositions.

Relaxor type ferroelectric compounds have a ferroelectric phase transition which encompasses a wide temperature range which results in broad peak in the dielectric constant when plotted as function of temperature. This phenomenon is described as a diffuse phase transition.² For capacitor applications this behaviour is advantageous since it yields a high dielectric constant over a wide temperature range. Lead magnesium niobate has been found to exhibit the highest dielectric constant and the lowest dissipation factor among the ferroelectric relaxor compounds¹. The maximum dielectric constant reported is 9,000 to 15,000 for the polycrystalline and monocrystalline forms, respectively.³ Recent studies have reported dielectric constants as high as 31,000 for the P_3MN - PT solid solutions.⁴

For relaxor type ferroelectrics, an increase of frequency causes the maximum of dielectric constant to

decrease in amplitude and to shift in the direction of higher temperature. The magnitude of the maximum dissipation factor increases with increasing frequency. This frequency dependence of the dielectric properties was explained by earlier workers, who proposed that these materials consisted of chemically different regions which formed microdomains with differing Curie temperatures which broaden the transition point over a wide temperature range. The frequency dependence can be understood if it is assumed that the total dielectric constant (K_T) is composed of an induced (K_{ind}) and reorientation polarization portion (K_{or}). The former is caused by electron and ionic polarizability while the latter is caused by reorientation of the polar regions of domains as well as the migration of domain walls. The maxima of these two contributions are located at different temperatures. Thus the maximum of K_T lies between the maxima of K_{ind} and K_{or} . As the frequency of the applied alternating field increases, the K_{or} is decreased while the K_{ind} remains unchanged, and as a consequence the maximum of the total dielectric constant is shifted towards that of K_{ind} as the contribution of K_{or} to K_T diminishes.

For capacitor applications the maximum of the dielectric constant is preferred to be at room temperature. The Curie temperature of P_3MN is located at $-15^{\circ}C$ ¹ which is too low for any practical purpose. In order to increase the Curie temperature, Ouchi et al⁵ added $PbTiO_3$ (PT) to P_3MN . Both Ouchi⁵ and Furukawa⁴ have shown that a composition of 92/8

P_3MN/PT weight fraction ratio yields a Curie temperature of 35°C .

It has been difficult to fabricate pure P_3MN by solid state reaction. An undesirable pyrochlore phase is generally formed along with the desired perovskite P_3MN . The exact composition of this undesirable pyrochlore phase is not completely defined as several compositions have been suggested, $Pb_3Nb_4O_{13}$ ⁶, $Pb_3Nb_4O_{13}$ with a little MgO ⁷, and $Pb_{1.83}Mg_{0.29}Nb_{1.71}O_{6.39}$ ⁸. It is evident that the undesirable pyrochlore is enhanced by the decreased reactivity of MgO at low temperatures and the loss of PbO at higher temperatures. At low temperatures, PbO tends to react with Nb_2O_5 to form $Pb_3Nb_4O_{13}$ because the reactivity of MgO at these temperatures is insignificant. As the temperature is increased, $Pb_3Nb_4O_{13}$ tends to react with both PbO and MgO to form the ternary pyrochlore phase. There might not be sufficient PbO to obtain stoichiometric P_3MN due to the loss of PbO at high temperatures.

Swartz⁷ showed that the problem of low reactivity of MgO could be avoided by reacting MgO with Nb_2O_5 to form $MgNb_2O_6$. The compound $MgNb_2O_6$ has a columbite structure with oxygen octahedra similar to the perovskite structure of P_3MN . By reacting PbO with $MgNb_2O_6$, nearly pure perovskite P_3MN can be obtained as long as the loss of PbO is minimized.

In order to minimize PbO loss, it is desirable to process

P_3MN at the lowest possible temperatures. It has been shown that considerable PbO loss occurs at temperatures above $1000^\circ C$. Thus, processing temperatures below $1000^\circ C$ are desirable.

It is known that there is a eutectic at $838^\circ C$ in the $PbO-PbTiO_3$ system⁹ and at about $840^\circ C$ in $PbO-Pb_3MgNb_2O_9$ system.¹⁰ It is likely that sintering in the presence of a small amount of PbO at temperatures above $840^\circ C$ will form a liquid phase, which will enhance densification. LeJeune¹¹ in fact has shown that densification is accelerated by the presence of excess PbO . Furukawa⁴ also found that the an excess MgO of 6 m% and 0.5 m% MnO in P_3MN -PT compositions inhibited the formation of the pyrochlore phase and increased the dielectric constant. The main objective of this research was to study the influence of excess PbO on the characteristics of P_3MN . Both MgO and MnO were also added since Furukawa⁴ showed these additives to be beneficial. The base composition used contained 70.7 m% P_3MN , 19.9 m% PT, and 9.4 m% MgO with 0.5 m% excess MnO . To minimize the formation of PbO crystals in the sintered structure the amount of excess PbO used was 1.7, 2.5 and 3.3 m% which was far less than the 21.8 m% used by LeJeune¹¹ in which case PbO crystals were observed.

The influence of sintering time and temperature on the density, microstructure, PbO loss and dielectric properties was investigated. To take advantage of the eutectic liquids the sintering temperatures used were 900, 950 and $1000^\circ C$. It

was anticipated that the sintering temperature could be lowered to around 950°C with the appropriate addition of PbO and still achieve superior dielectric properties for P₃MN-PT capacitors.

II. REVIEW OF LITERATURE

Lead magnesium niobate was first synthesized¹ by Smolenskii and Agranovskaya. These workers had earlier predicted¹² the formation of a group of complex compounds with perovskite type structures and solid solutions of these compounds. This prediction was based on the ionic radii, ionic valencies and the preferences of certain ions for a given coordination number.

Smolenskii et al.² have reported a study of those ferroelectrics and have observed diffuse phase transitions. They suggested that the diffuse phase transitions resulted from the composition fluctuations due to the random distributions of cations in their sublattice. Bokov and Myl'nikova³ synthesized single crystals of these compounds and also demonstrated¹³ the relaxation displacement phenomenon, i.e., the frequency dependence of the temperature of the dielectric maximum. Their explanation of the phenomenon also followed the lines of Smolenskii et al.².

Lead magnesium niobate was identified as being ferroelectric, piezoelectric and having the highest permittivity among those compounds investigated.^{1,14} Fritsberg et al.¹⁵ found that the perovskite P_3MN undergoes a rhombohedral distortion of the unit cell at the ferroelectric phase transition temperature rather than orthohombic as previously indicated by Bokov and Myl'nikova.¹⁴ Setter et al.¹⁶ later confirmed this finding by a study of the optical properties of the material.

Most of the investigations on P_3MN published before the 1980 dealt with its piezoelectric characteristics. These include the studies by Ouchi et al.^{5,17}, Bonner et al.¹⁸, Uchino et al.¹⁹, Jang et al.²⁰, Cross et al.²¹ and Nishido et al.²².

Ouchi⁵ has studied the P_3MN -PT solid solutions and evaluated the relation between the transition temperature and PT content. There appears to be a linear dependence between the transition temperature and the PT content. They also found a phase boundary at room temperature where a morphotropic transformation between the tetragonal phase (PT) and the pseudo-cubic phase (P_3MN) takes place. The phase boundary was found to be at 0.41 molar fraction of PT.

In 1982, Furukawa et al.⁴ published a study on use of P_3MN as a capacitor material. In this work, an optimum amount of excess MgO (about 6 m%) and MnO (0.5 m%) were added to eliminate the pyrochlore phase. This resulted in a maximum dielectric constant of 28,000. The samples were made by direct mixing of oxides and calcining at 800°C. The resulting powders were pressed and sintered in the temperature range 1000 to 1100°C. This study shows the potential of P_3MN -PT as a capacitor material.

An alternate method of P_3MN preparation was proposed by Swartz and Shrout⁷, in which, prior to reactions with PbO, the MgO and Nb_2O_5 were pre-reacted to form $MgNb_2O_6$. Excess MgO and PbO were then mixed with the $MgNb_2O_6$ and the mixture was calcined. A nearly pure perovskite P_3MN resulted. This processing sequence bypassed the formation of the pyrochlore

phase. They also reported that the pyrochlore phase formed had the chemical formula of $\text{Pb}_3\text{Nb}_4\text{O}_{13}$ with a small unknown amount of MgO in solid solution.

LeJeune and Boilot reported two studies^{6,23} dealing with the formation mechanism and the influence of ceramic processing on dielectric properties of P_3MN capacitors. The reaction product was identified as a mixture of P_3MN with a cubic perovskite type structure ($a=4.038 \text{ \AA}$) and another phase $\text{Pb}_3\text{Nb}_4\text{O}_{13}$ with the cubic pyrochlore type structure ($a=10.37 \text{ \AA}$). It was found that the dielectric properties of the products were highly dependent on the amount of pyrochlore phase present.

The dielectric properties of the ternary pyrochlore were reported by Shrout et al.⁸. They suggested that the cubic pyrochlore composition is $\text{Pb}_{1.83}\text{Mg}_{0.29}\text{Nb}_{1.71}\text{O}_{6.39}$ ($a=10.5988 \text{ \AA}$). The room temperature dielectric constant was found to be 130 which is consistent with the other pyrochlore type compounds. Swartz et al.²⁴ have studied the dielectric properties of P_3MN , P_3MN with excess MgO, P_3MN with deficient MgO as well as P_3MN -PT systems using the prereacted MgNb_2O_5 method that they described previously.⁷ They showed that as the grain size increases, the number of grain boundaries in series with the grains decreases, and that the high permittivity of pure P_3MN grains becomes less affected by the low permittivity grain boundaries. From this result, they concluded that either the addition of MgO or the increase of

sintering temperatures contribute to an increase in grain size which tends to increase the dielectric constant of the P_3MN capacitors.

In a comment on the grain size dependence of dielectric properties as suggested by Swartz et al.²⁴, Guha²⁵ has indicated that the residual grain boundary porosity present in the sintered ceramics might be more important than the grain size effect.

Chu and Hodgkins²⁶ published a study on the ultra low firing temperature ($950^{\circ}C$) for Y5U multilayer ceramic capacitors. By adding a flux as a sintering aid to the P_3MN -PT system, they achieved a dielectric constant of 15,000 for capacitors sintered at $950^{\circ}C$, which allows the use of Pd(<15%)/Ag(>85%) as internal electrodes.

LeJune et al.¹¹ used PbO as sintering aid to produce a liquid phase during sintering. With 21.8 m% PbO, a dielectric constant of 15,400 was obtained after sintering at $900^{\circ}C$ for 6 hours.

III. EXPERIMENTAL PROCEDURE

A. STARTING MATERIALS AND PREPARATION

A series of P₃MN-PT Compositions were prepared using PbO^{*}, MgNb₂O₅^{**}, MgO^{***}, PbTiO₃^{****} and MnO^{*****} powders as the starting materials.

The P₃MN- PT compositions with excess PbO were prepared by solid state reaction techniques. About 10 grams of PbO, MgNb₂O₅ and PbTiO₃ powders were first weighed, mixed in an agate mortar for about ten minutes, pressed into a compact at about 5 ksi and calcined in a closed alumina crucible for three hours at 750^o in air. Since the melting point of PbO is 886^oC, the calcination temperature has kept lower than this temperature to minimize the loss of PbO during the reaction. The closed alumina crucible also helped to minimize the PbO loss during this process.

* Yellow Cement Grade, Fisher Scientific Company

** TAM Ceramic Inc.

*** Electronic Grade, Fisher Scientific Company

**** TAM Ceramic Inc.

***** Apache Chemicals Inc.

After calcination the pellets were crushed into powders. This powder was used as the basic material for the subsequent preparation of the capacitors. To insure the completion of the reaction and to confirm that the pyrochlore phase content was minimized, the powders were analyzed by X-ray powder diffraction after calcination. Once the stoichiometric P_3MN formed, the loss of PbO from P_3MN -PT during sintering was too small to produce any noticeable amount of pyrochlore phase.

B. CAPACITOR PREPARATION AND SINTERING

About 6 grams of each composition was mixed with a few drops of polyvinyl alcohol - water solution. About 1.7 grams of the mixed powder was loaded into a 13mm diameter stainless steel die and pressed at about 40 ksi yielding a disc of about 2 mm in thickness.

Three discs were stacked on sintered P_3MN plates in an Al_2O_3 crucible which was covered with an Al_2O_3 lid. This tended to minimize the loss of PbO during sintering.

The crucible was first heated to $400^{\circ}C$ to remove the organic binder and then loaded into the furnace and heated in air from room temperature to the sintering temperature at a heating rate of $250^{\circ}C$ per hour and held at the desired sintering temperature for various periods. After cooling to room temperature the sintered discs were removed from the crucible and the properties were evaluated.

Two sets of samples were fabricated for each sintering temperature, time and amount of excess PbO addition to insure the reproducibility of the properties obtained in this study.

C. PHYSICAL PROPERTY MEASUREMENTS

The sintered samples were weighed for density, porosity, shrinkage and weight loss calculations. The diameter of the sintered discs was measured to the nearest 0.05 mm for the calculation of shrinkage.

The density of the sintered samples was measured using a buoyancy technique. The liquid was M-Xylene with a specific gravity around 0.865. The density was measured using a TiO₂ single crystal as a standard with a theoretical density of 4.26. M-Xylene was used as it does not react with the capacitor material and, after soaking for 15 minutes the pores of the disc become permeated with the liquid without heating. The reported data are the average of measurements made on two set of samples.

The weight loss was calculated from the difference in weight of the disc before and after sintering. Several samples were measured and the average value is reported.

D. DIELECTRIC AND ELECTRICAL PROPERTY MEASUREMENTS

Each capacitor was cleaned and then coated with In - Ga electrodes. Indium-Gallium forms a eutectic liquid slightly below room temperature so that an ohmic electrode can be easily formed on the surface of the capacitors.

The dielectric constant and dissipation factor at 1.0, 10, and 100 KHZ over the temperature range of -40°C to $+80^{\circ}\text{C}$ were measured. The capacitors were loaded into a tube furnace, were heated to 110°C in a partial vacuum for ten minutes to minimize water, then cooled to about -45°C by liquid nitrogen. The data were taken with a General Radio 1689 RLC bridge in conjunction with a Hewlett Packard HP-85 computer and Hewlett Packard 3497A Data Acquisition and Control Unit. The heating rate was 4°C per minute. The dielectric properties of the capacitors at T_c were measured after sintering by a HP 4270A Automatic Capacitance Bridge.

Electrical resistance was measured at the Curie temperature with a HP 4329A High Resistance Meter. The value reported was that of the capacitors which exhibited the best dielectric properties for each composition and sintering parameters (time and temperature).

The dielectric constant, dissipation factor and electrical resistivity data were reported as the average value of measurements made on two sets of samples.

E. X-RAY DIFFRACTION ANALYSIS

X-ray diffraction was used to check the purity of the P_3MN - PT powders. A General Electric XRD 700 X-Ray diffractometer was used in this study. The X-ray patterns were obtained using $CuK\alpha$ radiation over a 2θ range from 10° to 80° at a scanning rate of $2^\circ/\text{min}$. The undesired pyrochlore phase present after the calcination process can be readily identified by its characteristic peaks appearing in the diffraction pattern.

F. MICROSTRUCTURE DEVELOPMENT

The samples were broken into small pieces. Some of the broken samples were selected, mounted, and polished using No. 320, No. 400, No. 600 grinding papers and 5 and 1 μm alumina powders. The polished specimens were etched using a dilute HCl - HF - water solution. (19%-1%-80%) The microstructures of the fractured surfaces, sintered surfaces and polished sections were then examined by scanning electron microscopy (SEM) after coating with a conducting film.

For this purpose, a SEM (JOEL JMS 35C scanning electron microscope) was used in conjunction with an Energy Dispersive Spectrometer (EDS) to determine the composition of the specimens.

IV. RESULTS AND DISCUSSION

A. REACTIONS AND PHASE EQUILIBRIA

One of the problems with P_3MN - PT dielectric ceramics is the difficulty in producing a material consisting of only the perovskite phase. Depending on the processing conditions, a second phase with the pyrochlore structure is formed which has an adverse effect on the dielectric properties of the resulting material.

In the present investigation, solid state reactions between the precursor oxides (PbO , MgO and Nb_2O_5), and those between prefabricated $MgNb_2O_6$ and PbO were studied at temperatures up to $850^\circ C$. Since PbO melts congruently at $887^\circ C$, the reaction temperatures were limited to below the melting point of PbO .

Figure 1(A) shows the X-ray diffraction pattern resulting from the direct reaction between the constituent oxides, $PbO - MgO - Nb_2O_5$. As can be seen from the peaks marked PY, large quantities of the pyrochlore phase formed. Figures 1(B) and 1(C) are X-ray patterns resulting from using the $MgNb_2O_6$ and PbO reaction as was suggested by Swartz et al.¹⁸. As can be seen, very little pyrochlore phase was observed even without the addition of excess MgO (fig. 1B). Essentially no pyrochlore phase was formed with the addition of excess MgO (fig. 1C).

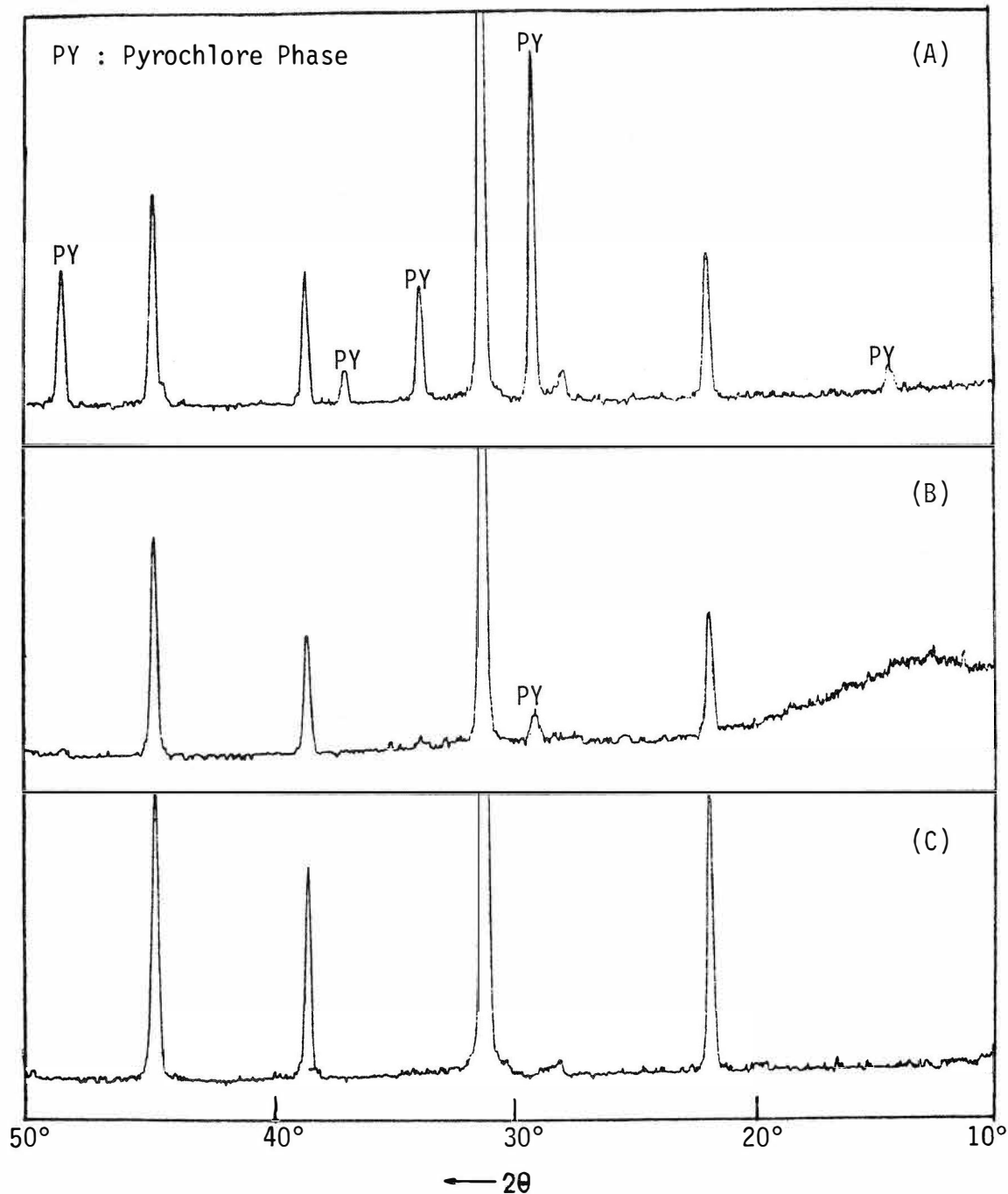


Figure 1 (A) X-Ray Diffraction Pattern Resulting from the Direct Reaction of $\text{PbO-MgO-Nb}_2\text{O}_5$ at 800°C .
 (B) X-Ray Diffraction Pattern Resulting from the Reaction of PbO and MgNb_2O_6 at 800°C .
 (C) X-Ray Diffraction Pattern Resulting from the Reaction of PbO and MgNb_2O_6 at 800°C with Excess MgO .

It is evident from these studies that a reaction between prefabricated MgNb_2O_6 and PbO with a small addition of excess MgO yields the best results. Thus for this study, this precalcined procedure as suggested by Swartz et al.¹⁸ was adopted.

X-ray diffraction patterns of the sintered samples indicated that both MgO and PbO are compatible with the perovskite $\text{P}_3\text{MN} - \text{PT}$ solid solution. Apparently, the addition of PbO to the solid solutions resulted in the formation of a liquid phase. Differential Thermal Analysis (DTA) traces obtained from different compositions showed that a sharp endothermic peak appeared at about 840°C which is a characteristic of melt formation. No other peak was found by DTA.

B. WEIGHT LOSS

The weight loss experiment was performed for various compositions at different sintering temperatures as a function of sintering time. The loss of PbO was found to influence both the sintering behaviour and the final properties of the P_3MN capacitors.

The weight loss of samples sintered at 900°C vs. sintering time is shown in figure 2. It can be seen that the excess PbO did not volatilize completely during sintering for

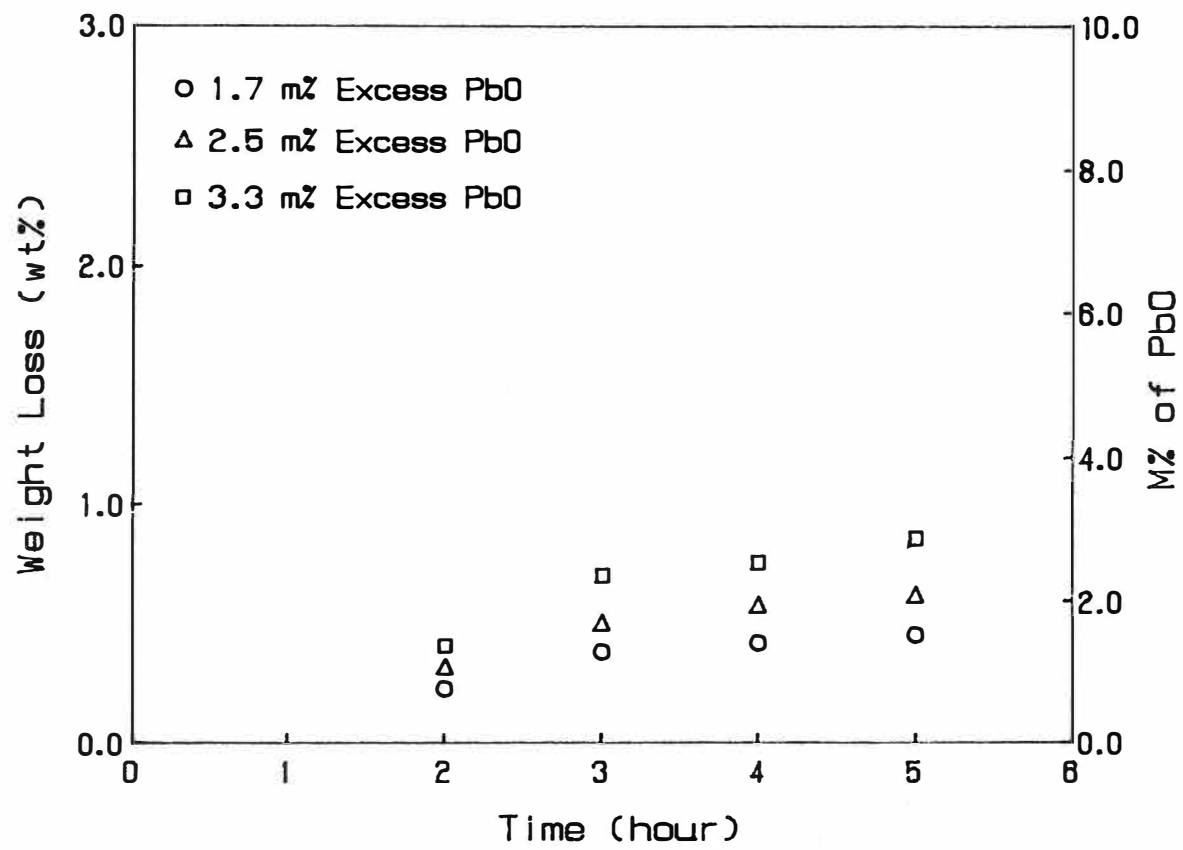


Figure 2. Weight Loss vs. Sintering Time for P_3MN-PT with Excess PbO Sintered at $900^\circ C$.

a period of three to five hours. This suggests that higher densities might be obtained in the presence of the liquid phase formed by the excess PbO. The amount of PbO should be kept to a minimum because its presence as a second phase in the capacitors is detrimental to the dielectric properties.

For those capacitors sintered at 950°C , the weight loss trends are shown in figure 3. The trends are analogous to the 900°C samples except that the weight loss became serious for sintering times exceeding four hours. The amount of loss is slightly larger due to the higher processing temperature. The PbO loss led to lower densification and formation of the pyrochlore phase. Therefore, in order to achieve the highest density and best dielectric properties, sintering times must be short enough to minimize the PbO loss. In this case, sintering times can not exceed five hours.

The weight loss trends for samples sintered at 1000°C are shown in figure 4. The weight loss at 1000°C is much higher than at either 900°C or 950°C . The sintering times must be short enough so that excessive PbO loss does not occur since the high PbO loss either shifts the composition of P_3MN phase or produces high porosity.

The fact that the weight loss increases with increasing excess PbO content at a given sintering temperature and time, as shown in figures 2, 3 and 4, seems to indicate that the presence of the liquid phase during sintering may induce the loss of PbO from the P_3MN -PT solid solution. This suggests that the higher amounts of liquid phase present increase the

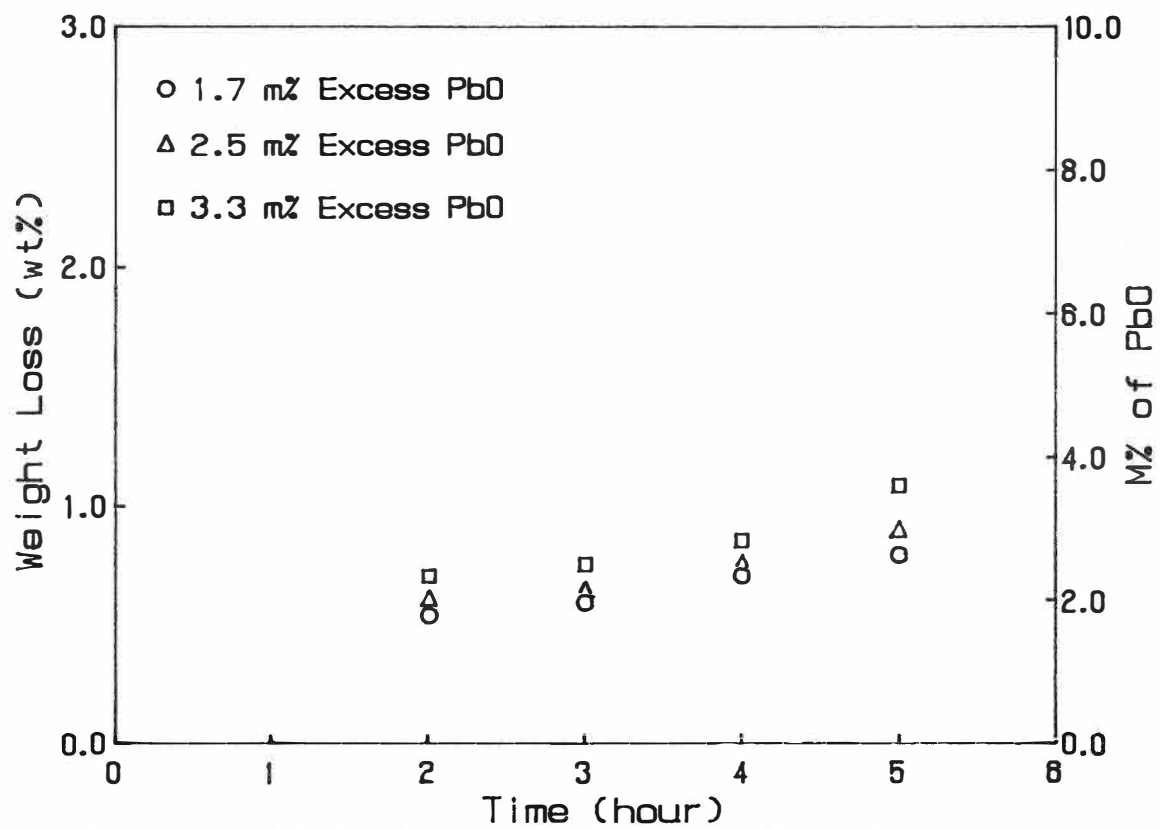


Figure 3. Weight Loss vs. Sintering Time for P_3MN-PT with Excess PbO Sintered at $950^\circ C$.

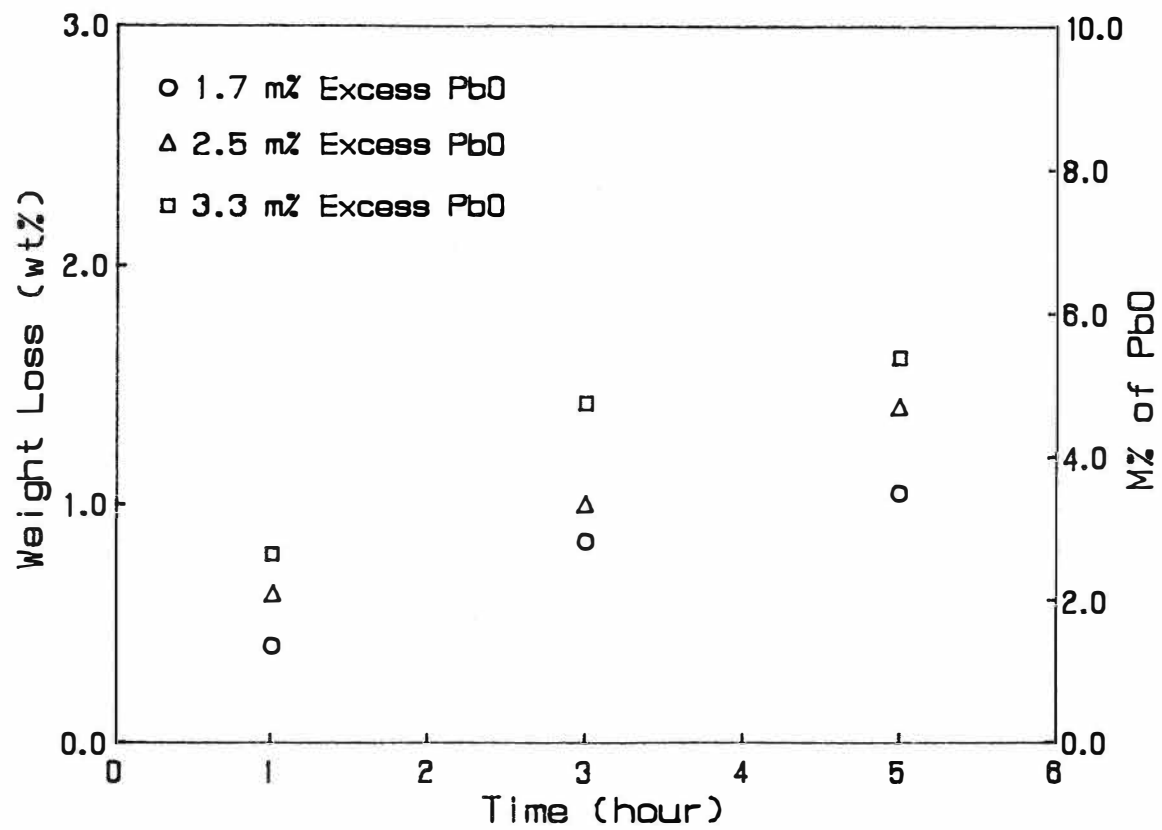


Figure 4. Weight Loss vs. Sintering Time for P_3MN-PT with Excess PbO Sintered at $1000^\circ C$.

PbO loss. Therefore, densification could be impeded by the enhanced PbO loss resulting from either higher sintering temperatures or increases in the excess PbO.

C. SINTERING CHARACTERISTICS

All of the densification data are contained in Appendix B. The data were obtained by measuring 2 sets of samples and are reported as an average value for each temperature, time and composition. The theoretical density of the P_3MN -PT base composition was calculated to be 8.07 g/cm^3 . The calculation is given in Appendix A.

The correlations between bulk density and weight loss data are shown in figures 5, 6 and 7 for sintering at 900, 950 and 1000°C , respectively. As can be seen in the figures, the highest density for each composition at a given sintering temperature was obtained where the amount of PbO loss is close to the amount of excess PbO added. Little of the liquid phase produced by the excess PbO was left in the specimens after sintering. It is apparent that the loss of PbO beyond the excess PbO added during sintering results in decreased densification. The bulk density is also low for those specimens with PbO loss far less than the excess PbO addition because the densification could not be completed and a second phase rich in PbO remains in the grain boundaries.

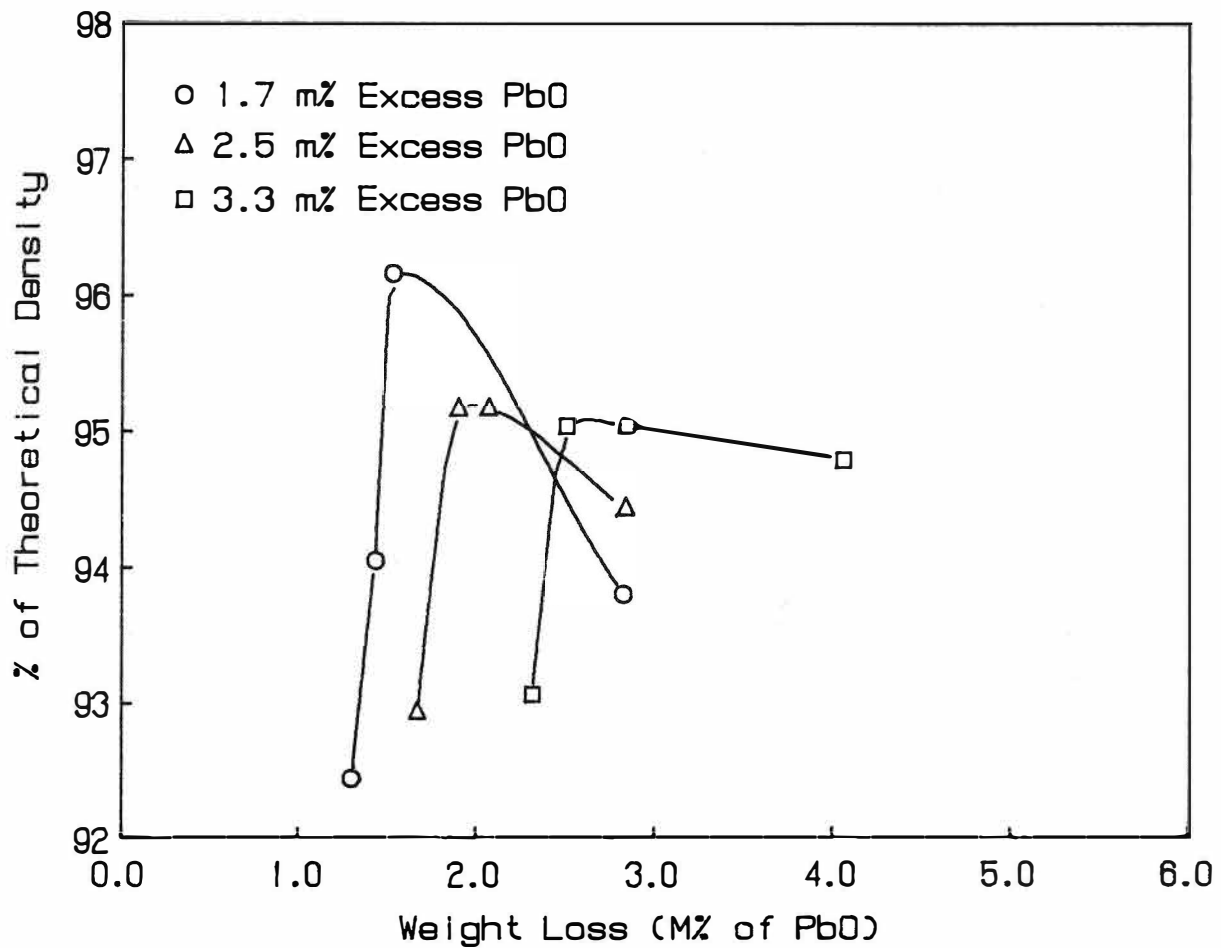


Figure 5. Density vs. Weight Loss for P_3MN -PT with Excess PbO Sintered at 900°C.

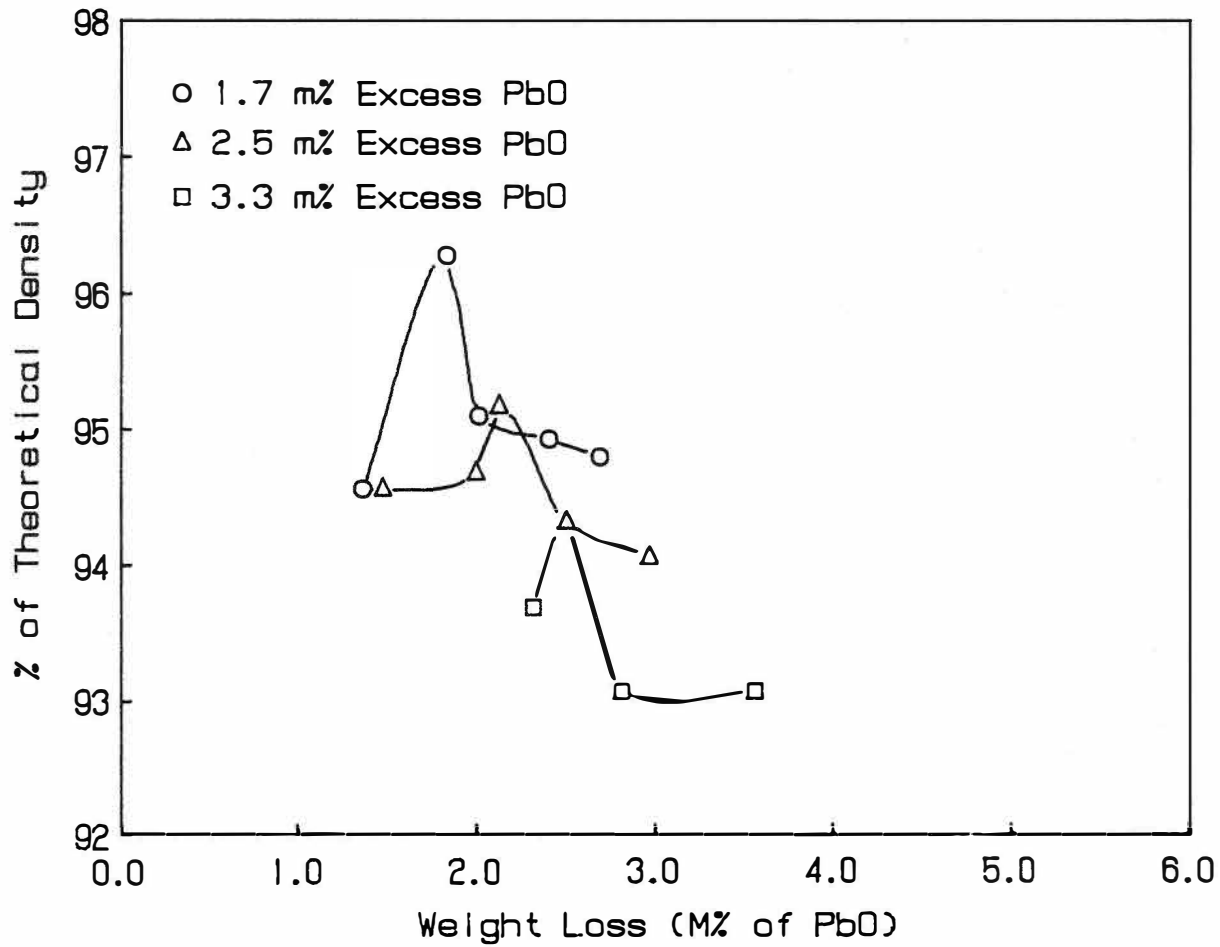


Figure 6. Density vs. Weight Loss for P_3MN -PT with Excess PbO Sintered at 950°C.

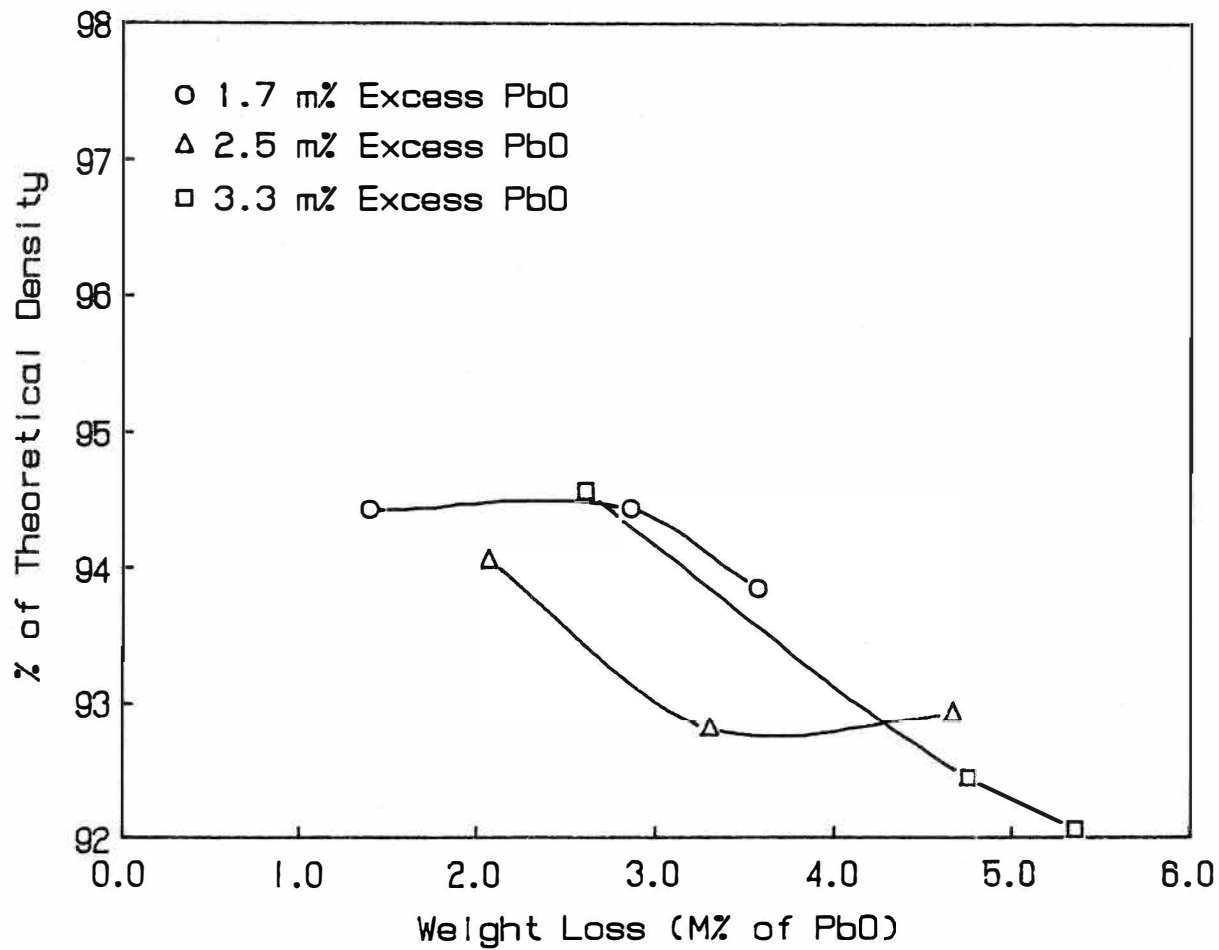


Figure 7. Density vs. Weight Loss for P_3MN -PT with Excess PbO Sintered at 1000°C.

The density data as % of theoretical density and the corresponding weight loss data as mol % of PbO vs. sintering temperature for times of 3h and 5h are shown in figures 8 and 9, respectively. As can be seen in figure 8, for sintering at 900°C for 3 h, the PbO loss was much lower than the excess PbO content. The specimens with higher PbO contents have higher bulk densities because higher amounts of liquid phase were produced during sintering. For sintering at 950°C for 3 h the PbO loss increased as compared with those at 900°C. However, the PbO loss was still below the excess PbO content. Therefore, higher bulk densities were obtained at 950°C than at 900°C due to the higher processing temperature. The PbO loss was so high when sintering at 1000°C for 3h that densification was impeded. Also, as shown in figure 8, the PbO loss increases with increasing excess PbO content. As a result, the higher the excess PbO added the lower the final density.

For 5h sintering at 900, 950 and 1000°C, higher densities were obtained for the lower excess PbO content, as shown in figure 9. Also, the densification is worse for sintering of 5h than for 3h except for those sintered at 900°C where the PbO losses were less than the amount of excess PbO. As a result, the bulk density decreases with increasing sintering temperature for 5h of sintering.

From figures 8 and 9, it appears that a low sintering temperature (900°C) and PbO content (1.7 m%) may yield densities in excess of 96% of theoretical density.

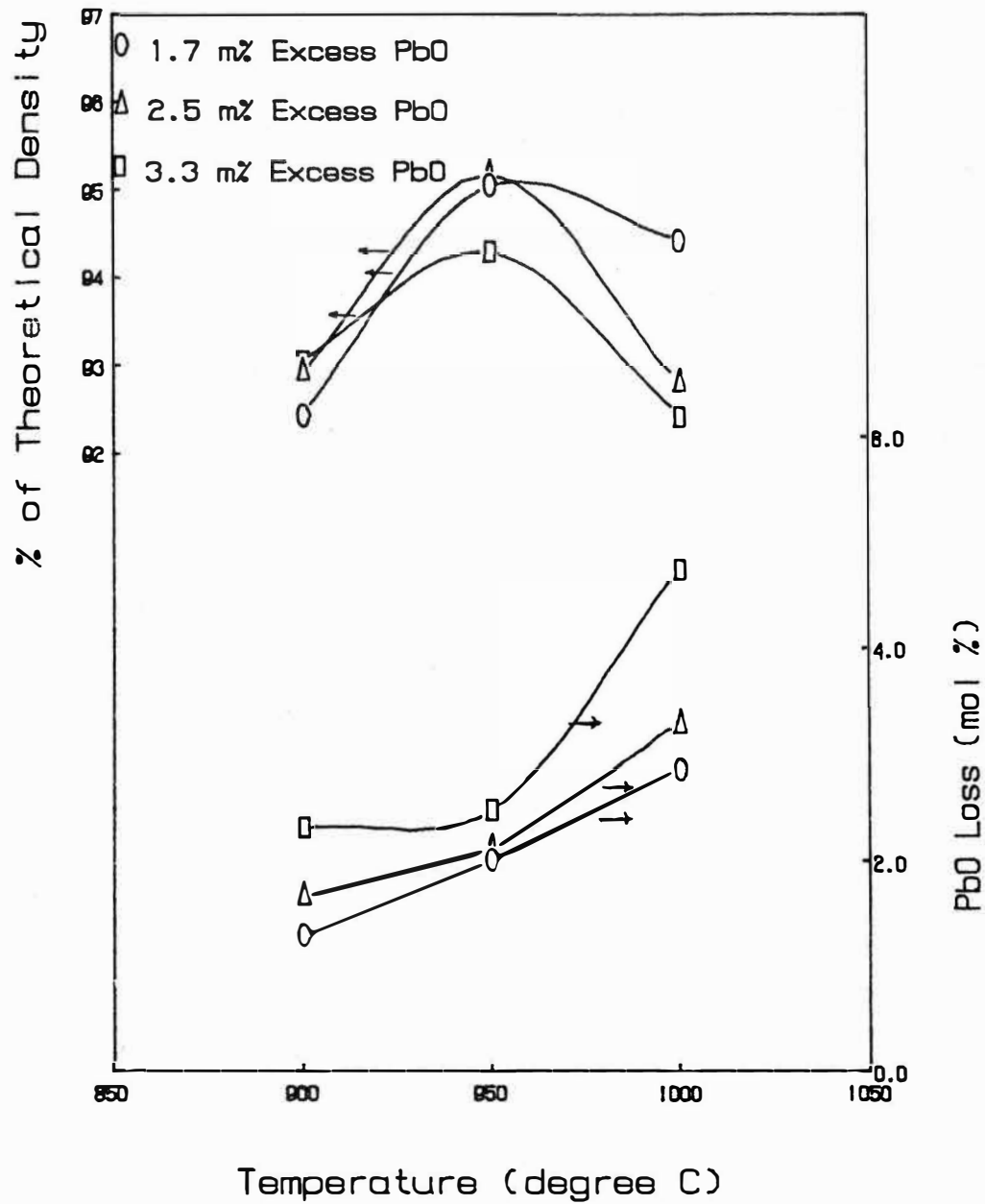


Figure 8. Density and Weight Loss vs. Sintering Temperature for P_3MN-PT with Excess PbO Sintered for 3h.

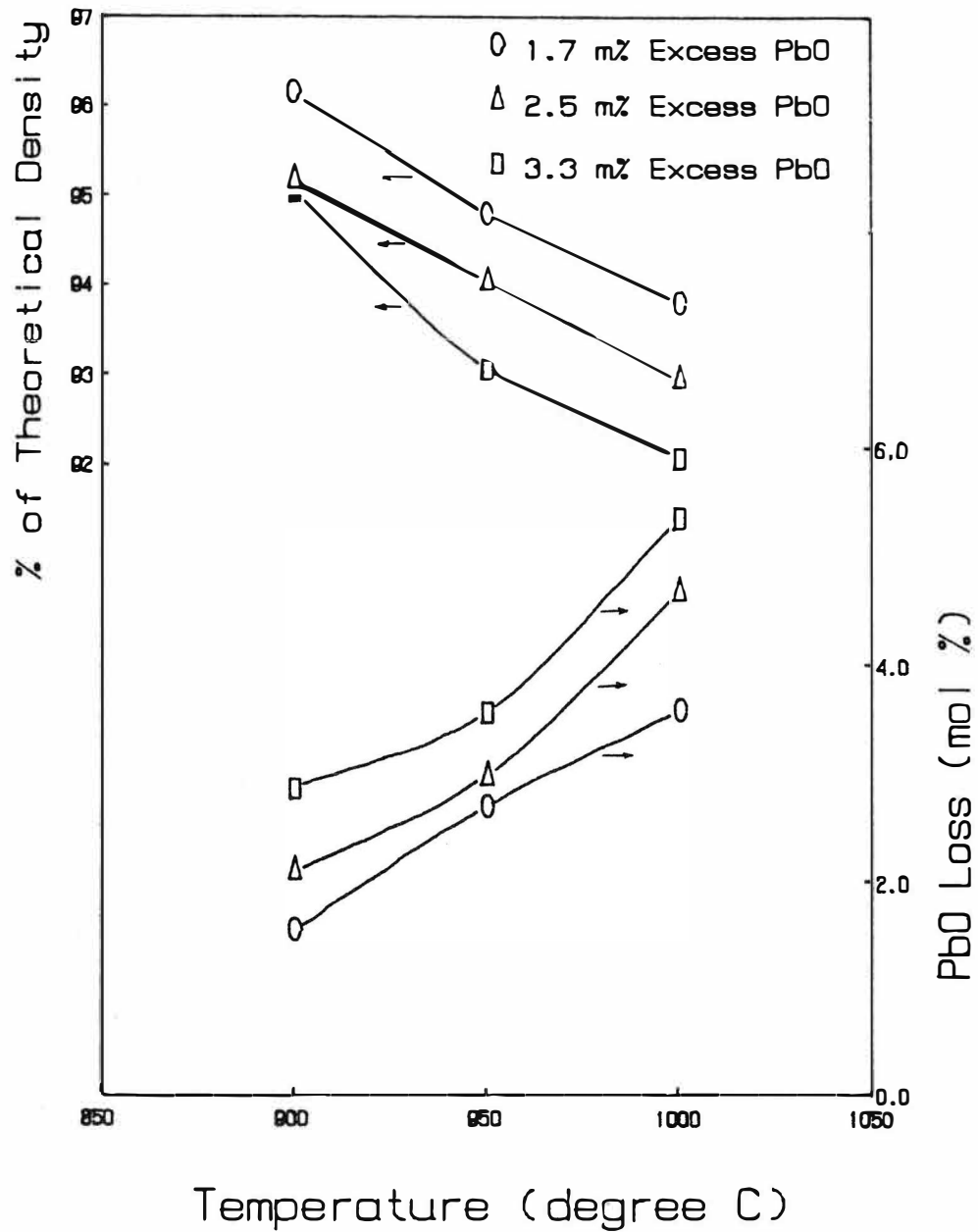


Figure 9. Density and Weight Loss vs. Sintering Temperature for P_3MN-PT with Excess PbO Sintered for 5h.

D. MICROSTRUCTURES

The sintered and fracture surfaces of specimens with 2.5 m% excess PbO sintered at 950°C were examined with the scanning electron microscope. Figure 10 shows the fracture surface of a specimen sintered for 1h. A number of flake-like PbO crystals (which were identified by Energy Dispersive Spectrometer (EDS)) can be seen as a second phase. This shows that insufficient PbO volatilization occurred to remove the excess PbO from the structure. The weight loss data suggests that only 40 % of the excess PbO volatilized from the structure.

As shown in figure 11 crystals of PbO can also be seen on the sintered surfaces. Again this suggests that excess PbO existed in the system after sintering.

Figures 12 and 13 show the sintered and fracture surfaces of a specimen sintered at 950°C for 3 h. No PbO crystals were seen in the microstructure, showing that most of the excess PbO had been volatilized. As can be seen in fig. 4, the PbO loss is close to 2.5 m%, leaving a dense, low porosity structure.

Figure 14 shows a fracture surface of a specimen containing 2.5 m% excess PbO sintered at 950°C for 3h which displays evidence of a liquid phase. The weight loss data suggests that about 15% of the excess PbO remains. The rounding of the surfaces of the grains also implies the presence of liquid phase during sintering.

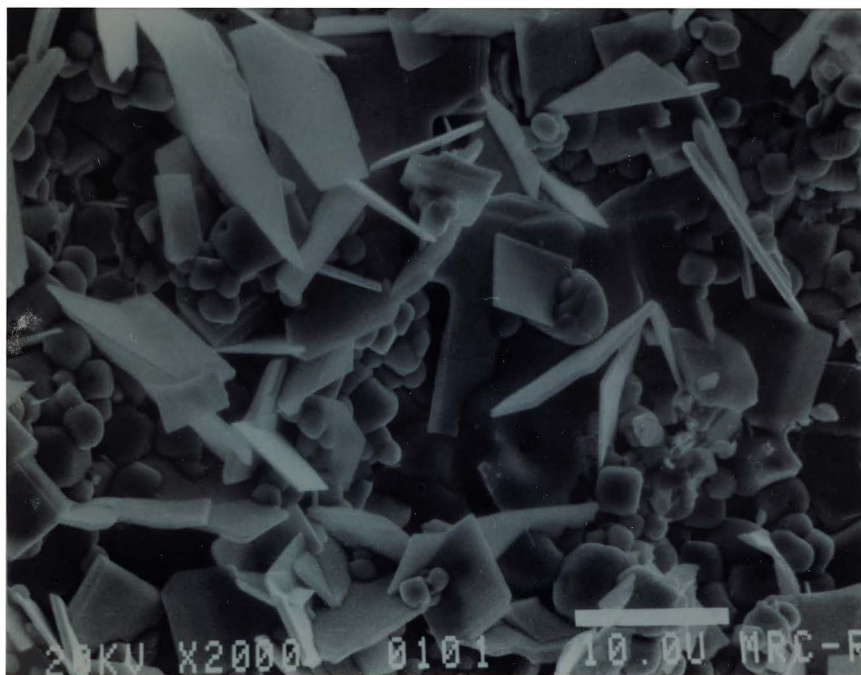


Figure 10. SEM Photomicrograph of a Fracture Surface of P_3MN -PT with 2.5 m% Excess PbO Sintered for 1h at 950°C. (PbO Loss: 1.47 m%)

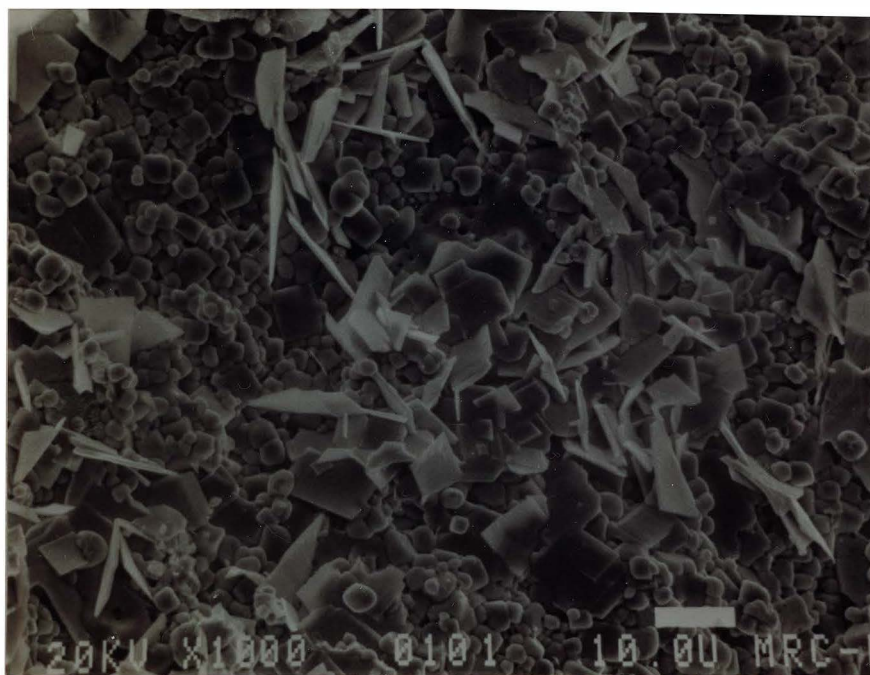


Figure 11. SEM Photomicrograph of a Sintered Surface of P_3MN -PT with 2.5 m% Excess PbO Sintered for 1h at 950°C. (PbO Loss: 1.47 m%)

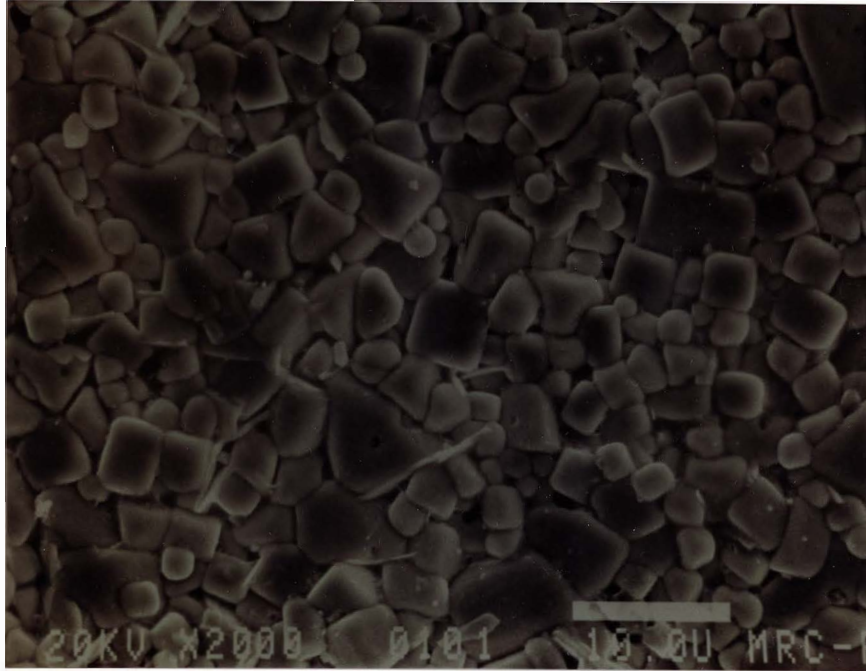


Figure 12. SEM Photomicrograph of a Sintered Surface of P₃MN-PT with 2.5 m% Excess PbO Sintered for 3h at 950°C. (PbO Loss: 2.13 m%)

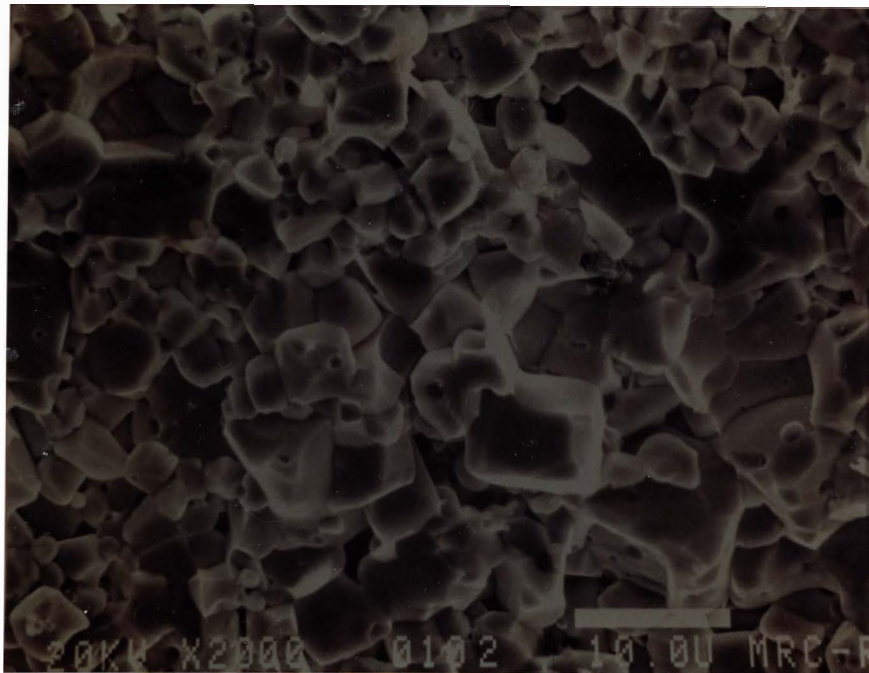


Figure 13. SEM Photomicrograph of a Fracture Surface of P₃MN-PT with 2.5 m% Excess PbO Sintered for 3h at 950°C. (PbO Loss: 2.13 m%)

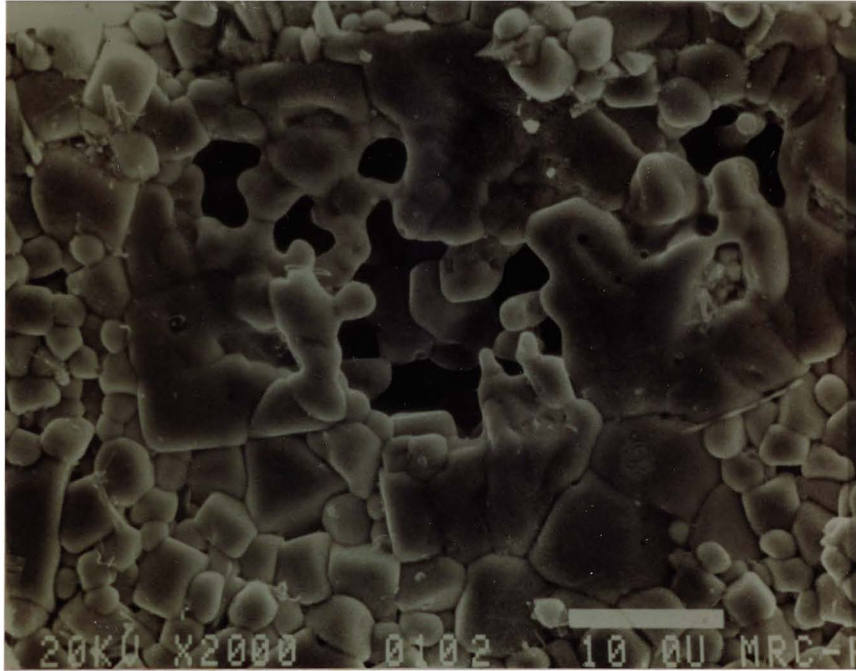


Figure 14. SEM Photomicrograph of a Fracture Surface of P_3MN -PT with 2.5 m% Excess PbO Sintered for 3h at 950°C. (PbO Loss: 2.13 m%)

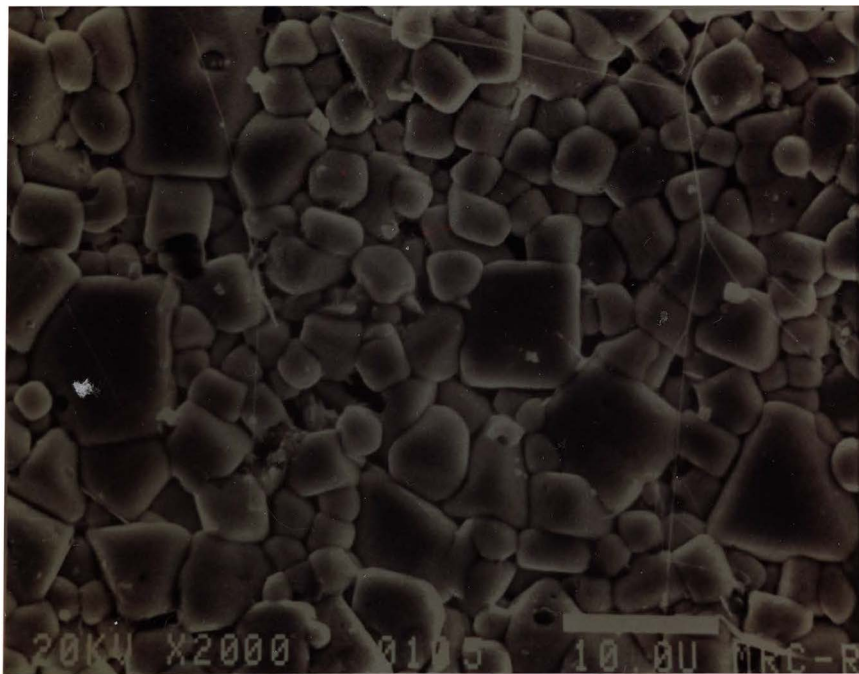


Figure 15. SEM Photomicrograph of a Sintered Surface of P_3MN -PT with 2.5 m% Excess PbO Sintered for 5h at 950°C. (PbO Loss: 2.63 m%)

Figures 15 and 16 are photomicrographs of a specimen with 2.5 m% excess PbO sintered at 950°C for 5 h. Regions of abnormal grain growth with pores trapped inside the grains can be observed. The weight loss data shows that about 3 m% PbO was lost from the specimen so that some of the PbO had to volatilize from the solid solution, which decreased the sintered density.

Thus it appears that high densities are obtainable without either PbO crystals formed as a second phase or the loss of structural PbO through the PbO-rich liquid phase if sintering time and temperature are appropriately controlled.

The influence of excess MgO in the base composition can be seen in figure 17. This is a fracture surface of a specimen with 9.4 m% excess MgO and 3.3 m% excess PbO sintered at 950°C for 2 h. As indicated in this photomicrograph, the small round spots on the boundaries of the large grains are MgO particles (identified by EDS). The presence of MgO particles was observed in the fracture surface of all the specimens examined by the SEM.

The photomicrograph of a fracture surface of a specimen with 3.3 m% PbO sintered at 1000°C for 1 h is shown in figure 18. As can be seen the grain growth was promoted more at 1000°C than at 950°C, probably from the presence of the larger amount of liquid phase. The weight loss data shows that for 1 hour of sintering, at least 0.7 m% excess PbO remains in the structure.

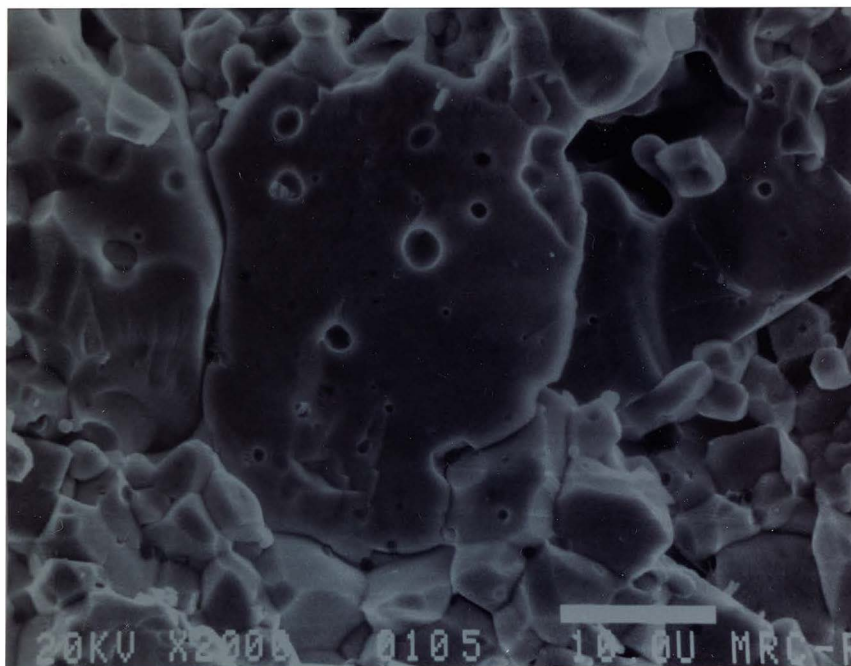


Figure 16. SEM Photomicrograph of a Fracture Surface of P_3MN-PT with 2.5 m% Excess PbO Sintered for 5h at $950^{\circ}C$. (PbO Loss: 2.63 m%)

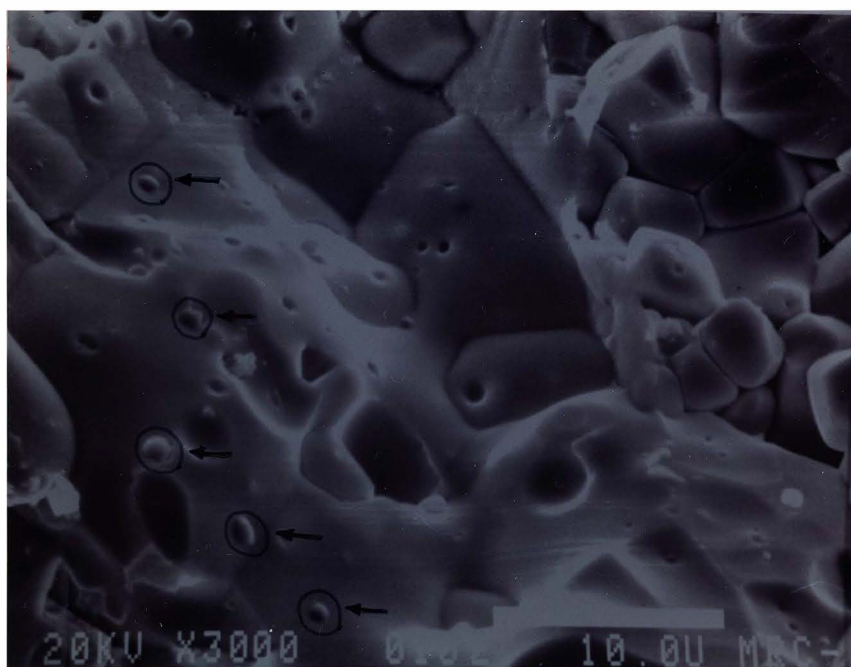


Figure 17. SEM Photomicrograph of a Fracture Surface of P_3MN-PT with 3.3 m% Excess PbO Sintered for 2h at $950^{\circ}C$. (MgO ←)

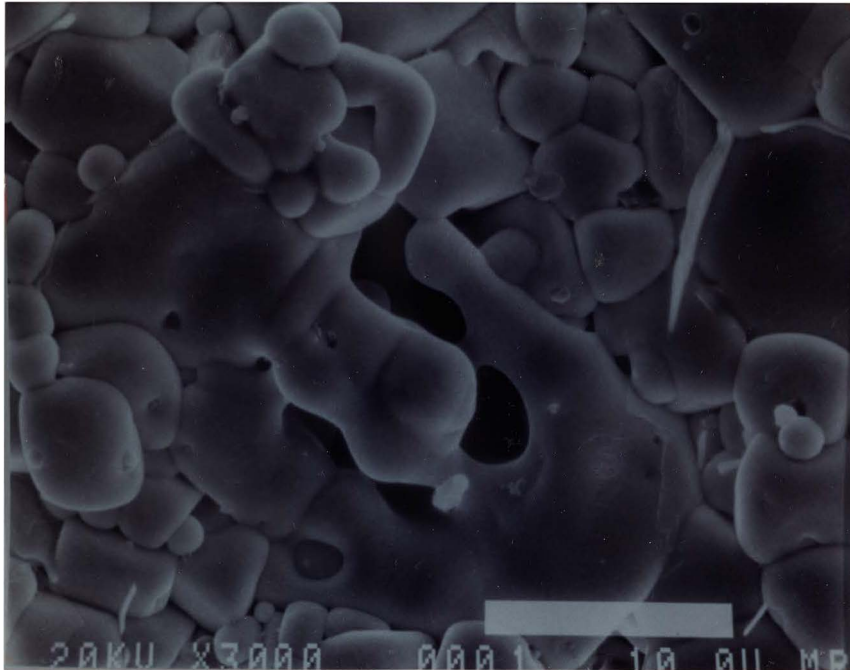


Figure 18. SEM Photomicrograph of a Fracture Surface of P_3MN-PT with 3.3 m% Excess PbO Sintered for 1h at $1000^{\circ}C$. (PbO Loss: 2.6 m%)

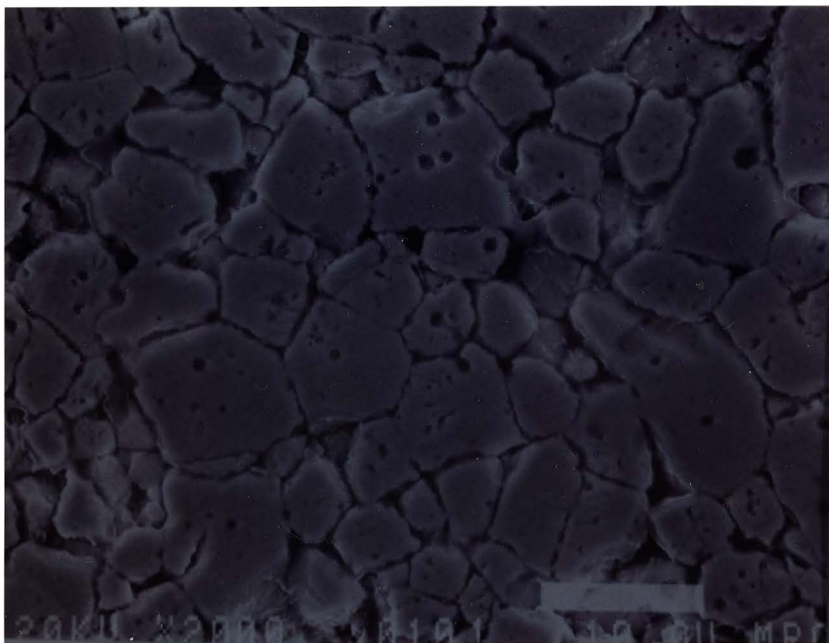


Figure 19. SEM Photomicrograph of a Polished and Etched Section of P_3MN-PT with 3.3 m% Excess PbO Sintered for 1h at $1000^{\circ}C$. (PbO Loss: 2.6 m%)

Figures 19, 20 and 21 are photomicrographs of polished sections for specimens with 3.3 m% excess PbO sintered at 1000°C for 1 h, 2 h and 3 h, respectively. As can be seen in these figures the amount of liquid phase contained in the grain boundaries decreases with increasing sintering time. This is due to the PbO loss which leaves vacant grain boundaries and higher porosity in the microstructure as shown in figure 21. The weight loss data shows that after 1, 2 and 3h, 2.6, 3.6 and 4.8 m% PbO, respectively were lost from the structure.

As compared with the microstructures obtained for less excess PbO addition and sintering at lower temperature which are shown in figure 12 and 13, the photomicrograph in figure 21 shows an enhanced grain growth, an increase of porosity, and a decrease in density. However, superior dielectric properties were obtained. This may be due to grain growth as discussed in the next section.

E. DIELECTRIC AND ELECTRICAL PROPERTIES

Figures 22 to 27 show the temperature dependence of the dielectric constant and dissipation factor for the capacitors with 3.3 m% excess PbO sintered for 3h at 900, 950 and 1000°C, respectively. As can be seen the capacitors exhibit the typical characteristics of relaxors in that the dielectric constant is frequency dependent and the Curie

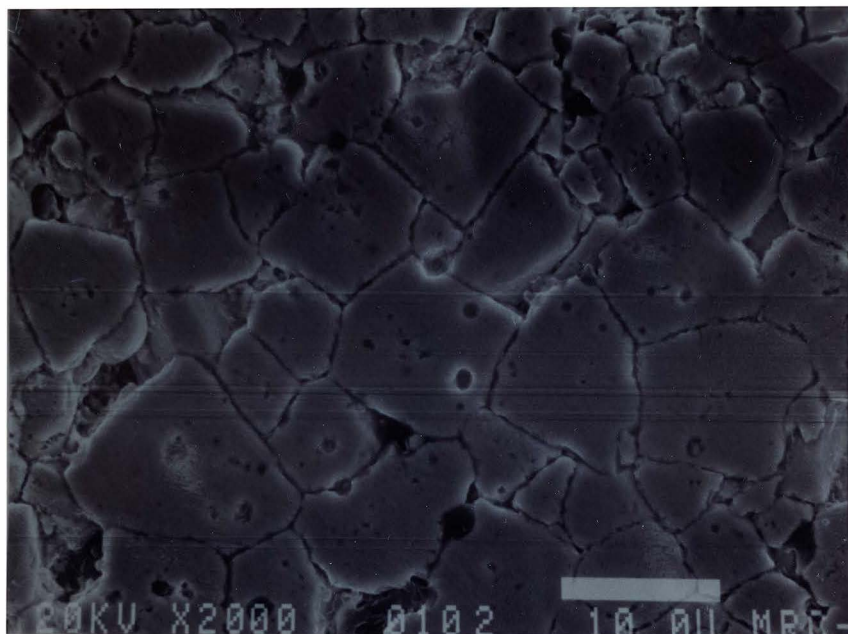


Figure 20. SEM Photomicrograph of a Polished and Etched Section of P_3MN-PT with 3.3 m% Excess PbO Sintered for 2h at $1000^{\circ}C$. (PbO Loss: 3.6 m%)

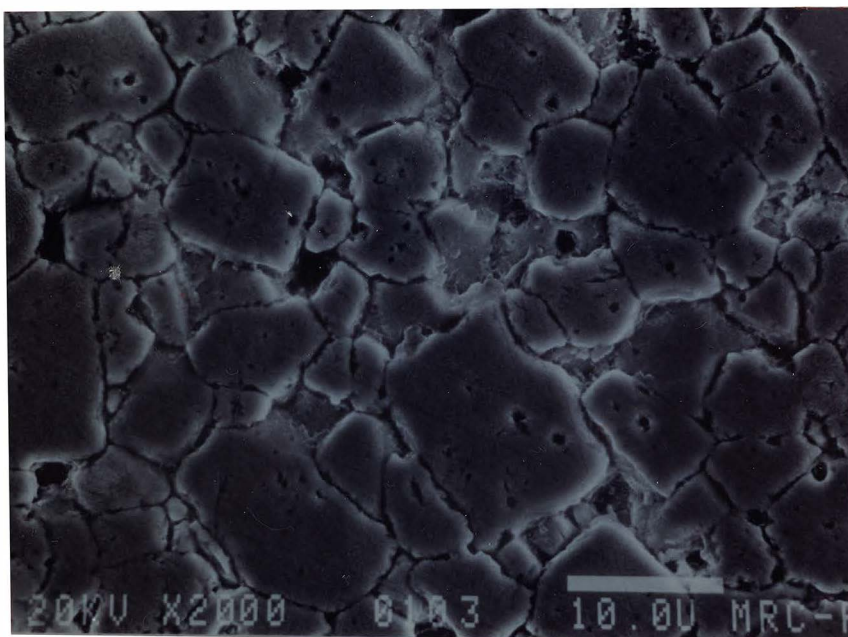


Figure 21. SEM Photomicrograph of a Polished and Etched Section of P_3MN-PT with 3.3 m% Excess PbO Sintered for 3h at $1000^{\circ}C$. (PbO Loss: 4.75 m%)

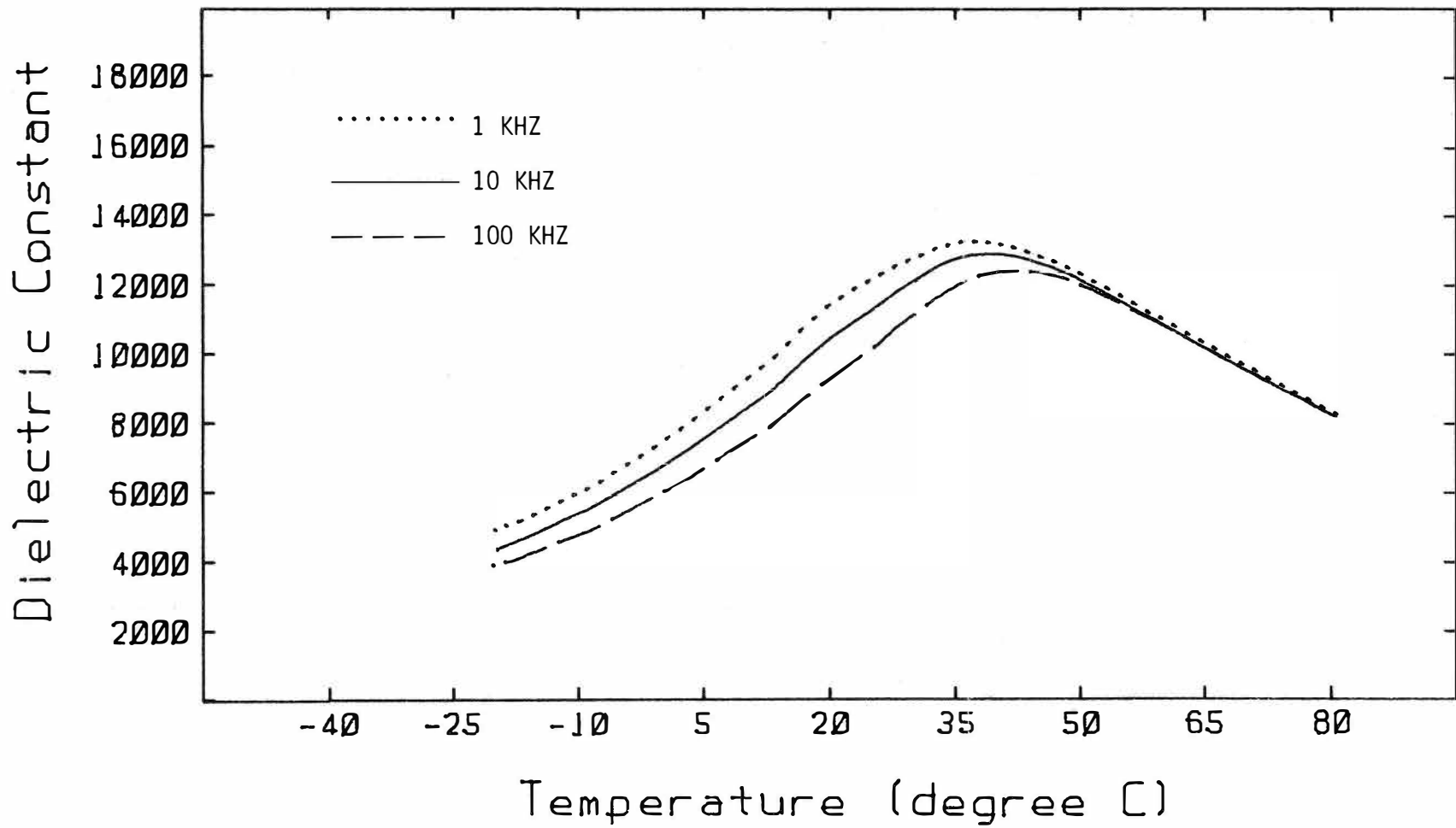


Figure 22. Dielectric Constant vs. Temperature for P_3MN -PT with 3.3 m% Excess PbO Sintered for 3 hours at $900^{\circ}C$.

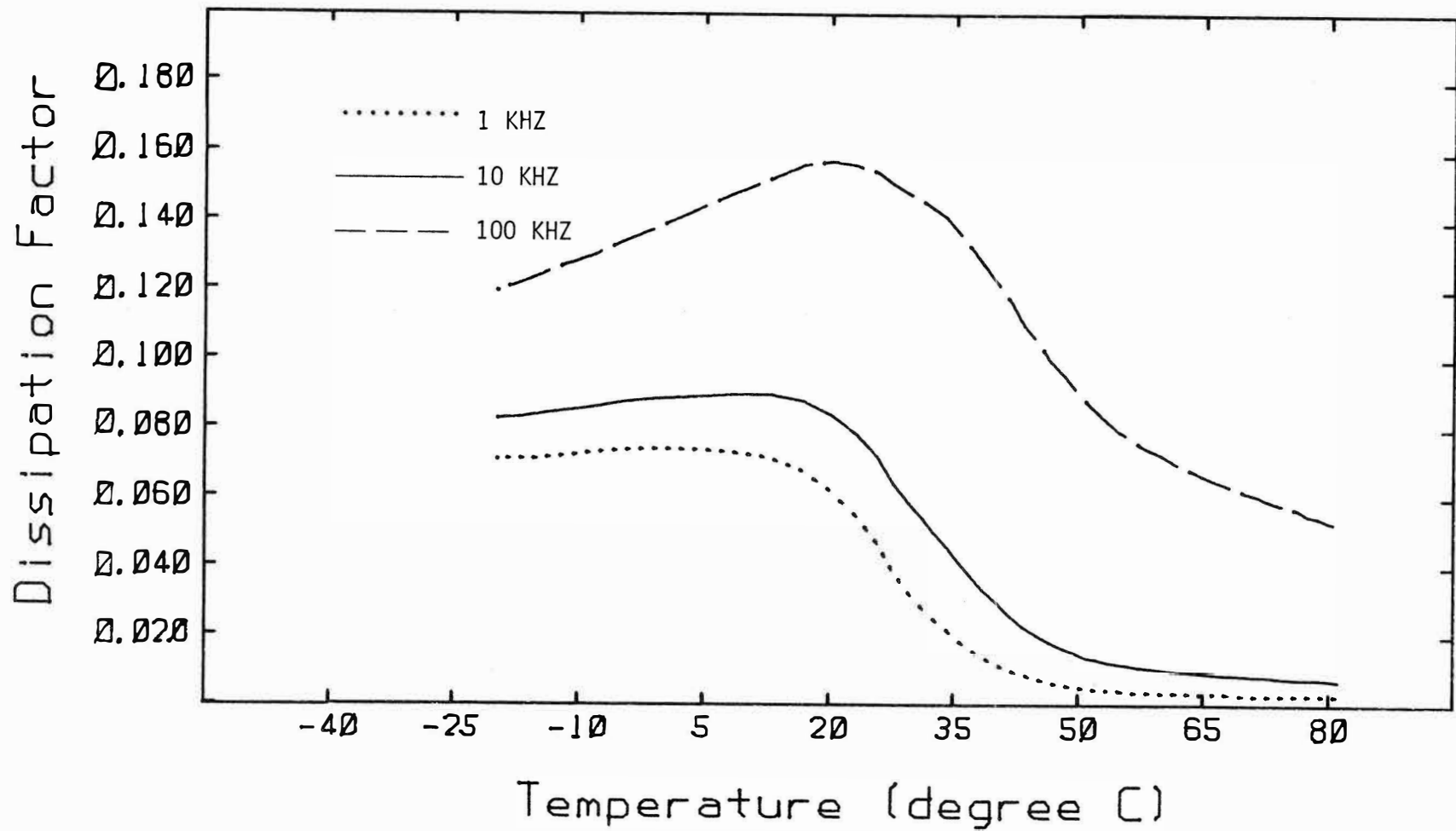


Figure 23. Dissipation Factor vs. Temperature for P_3MN -PT with 3.3 m% Excess PbO Sintered for 3 hours at $900^{\circ}C$.

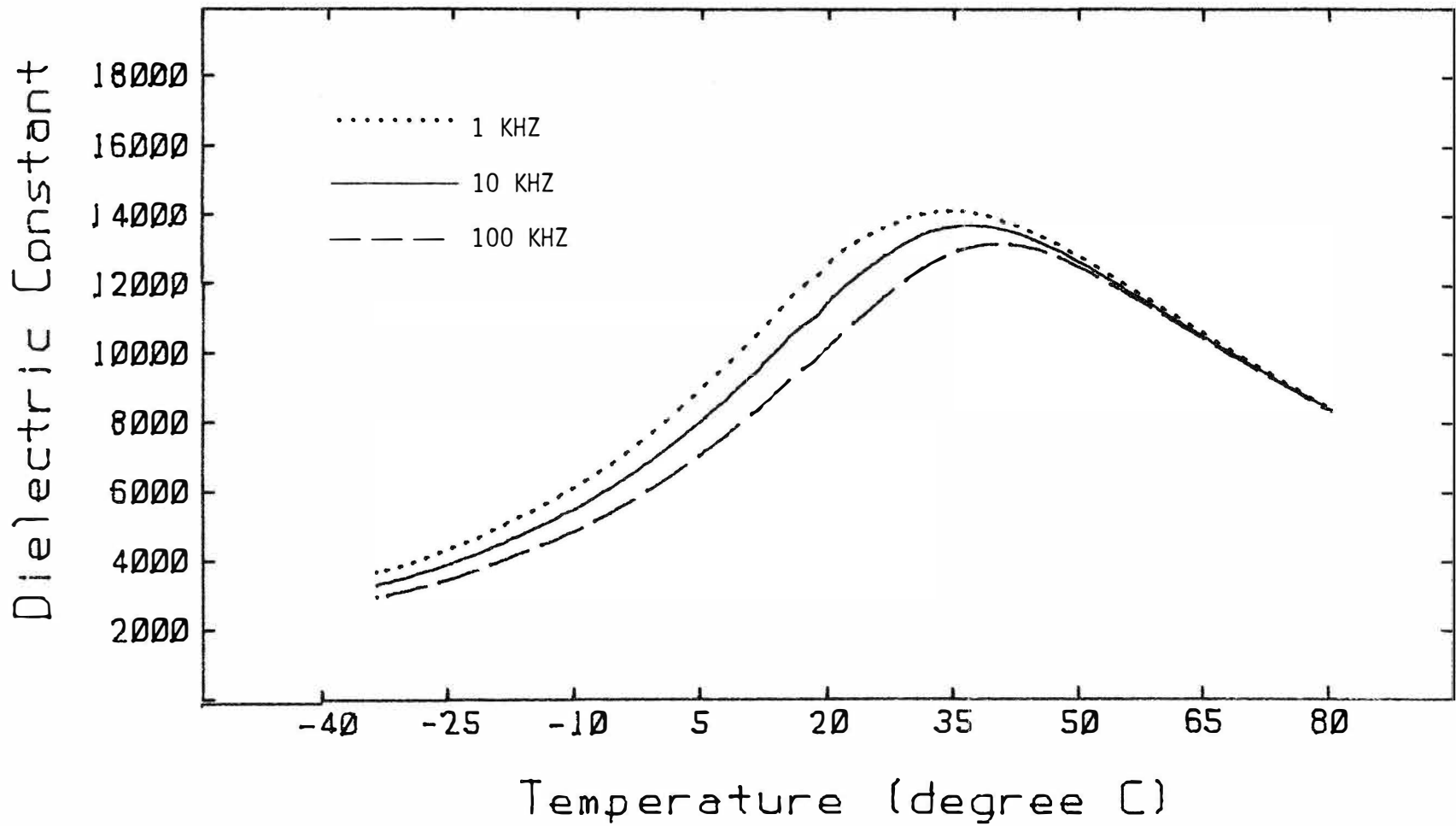


Figure 24 . Dielectric Constant vs. Temperature for P_3MN -PT with 3.3 m% Excess PbO Sintered for 3 hours at $950^{\circ}C$.

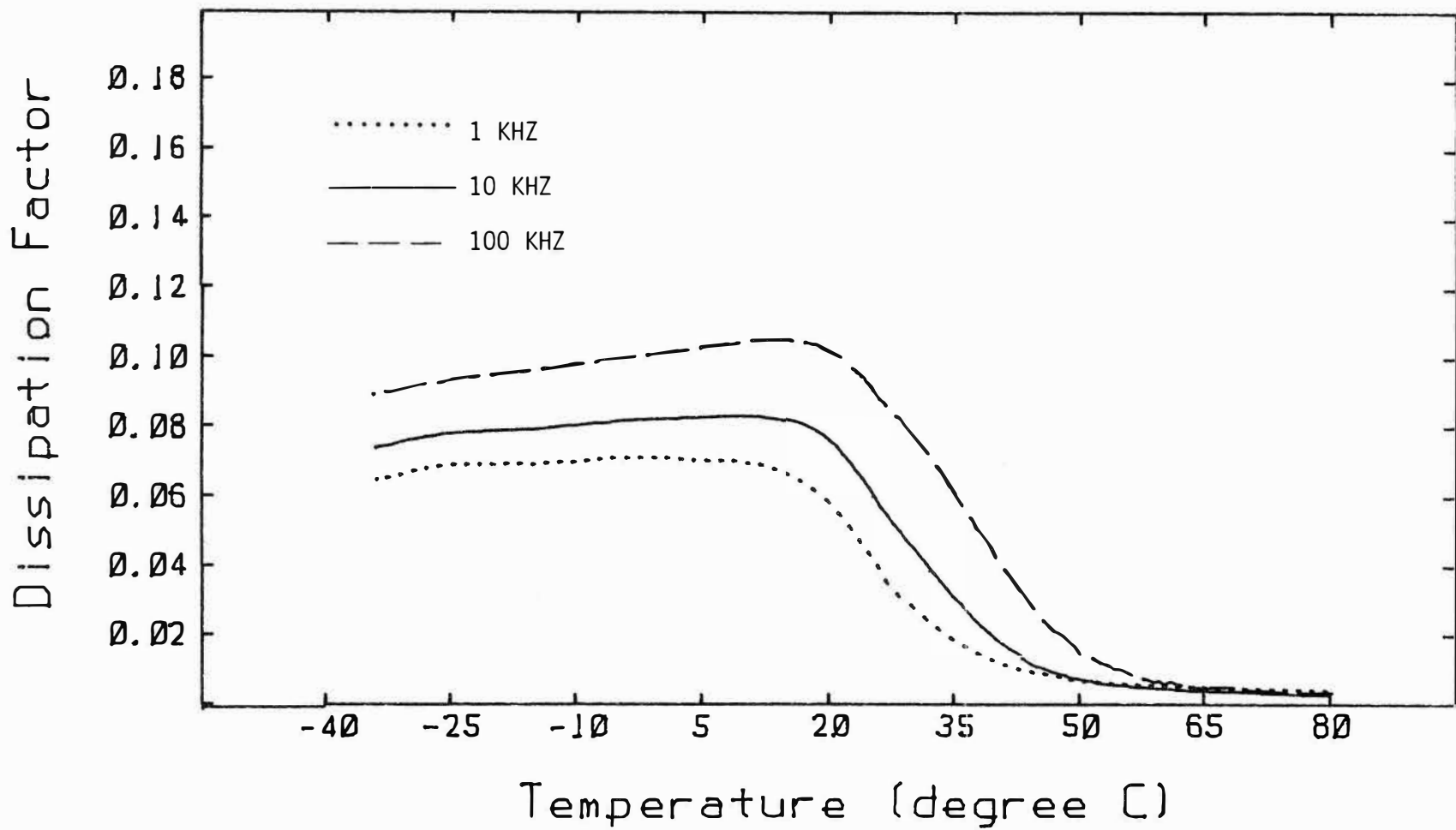


Figure 25. Dissipation Factor vs. Temperature for P_3MN-PT with 3.3 m% Excess PbO Sintered for 3 hours at $950^{\circ}C$.

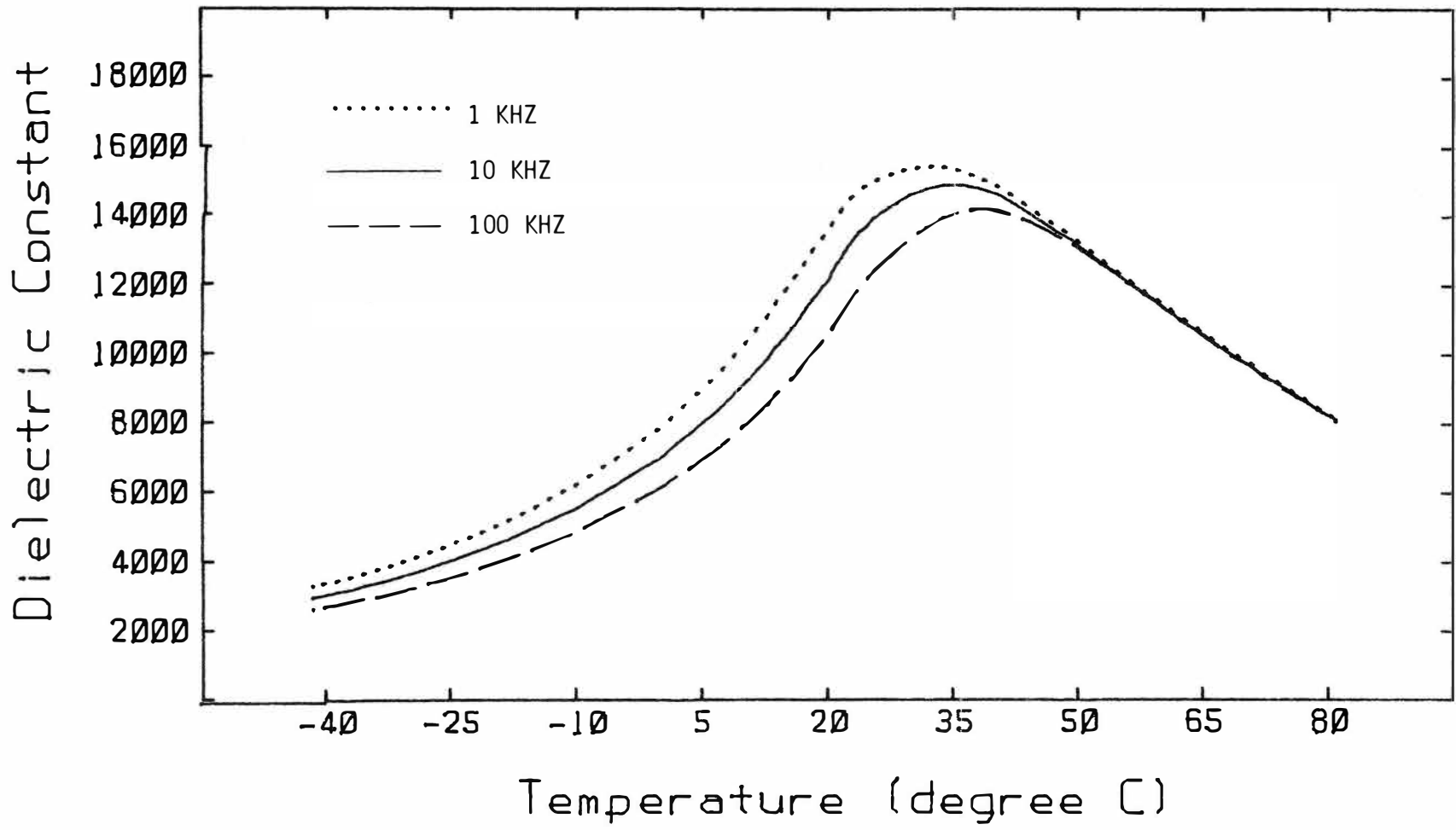


Figure 26. Dielectric Constant vs. Temperature for P₃MN-PT with 3.3 m% Excess PbO Sintered for 3 hours at 1000°C.

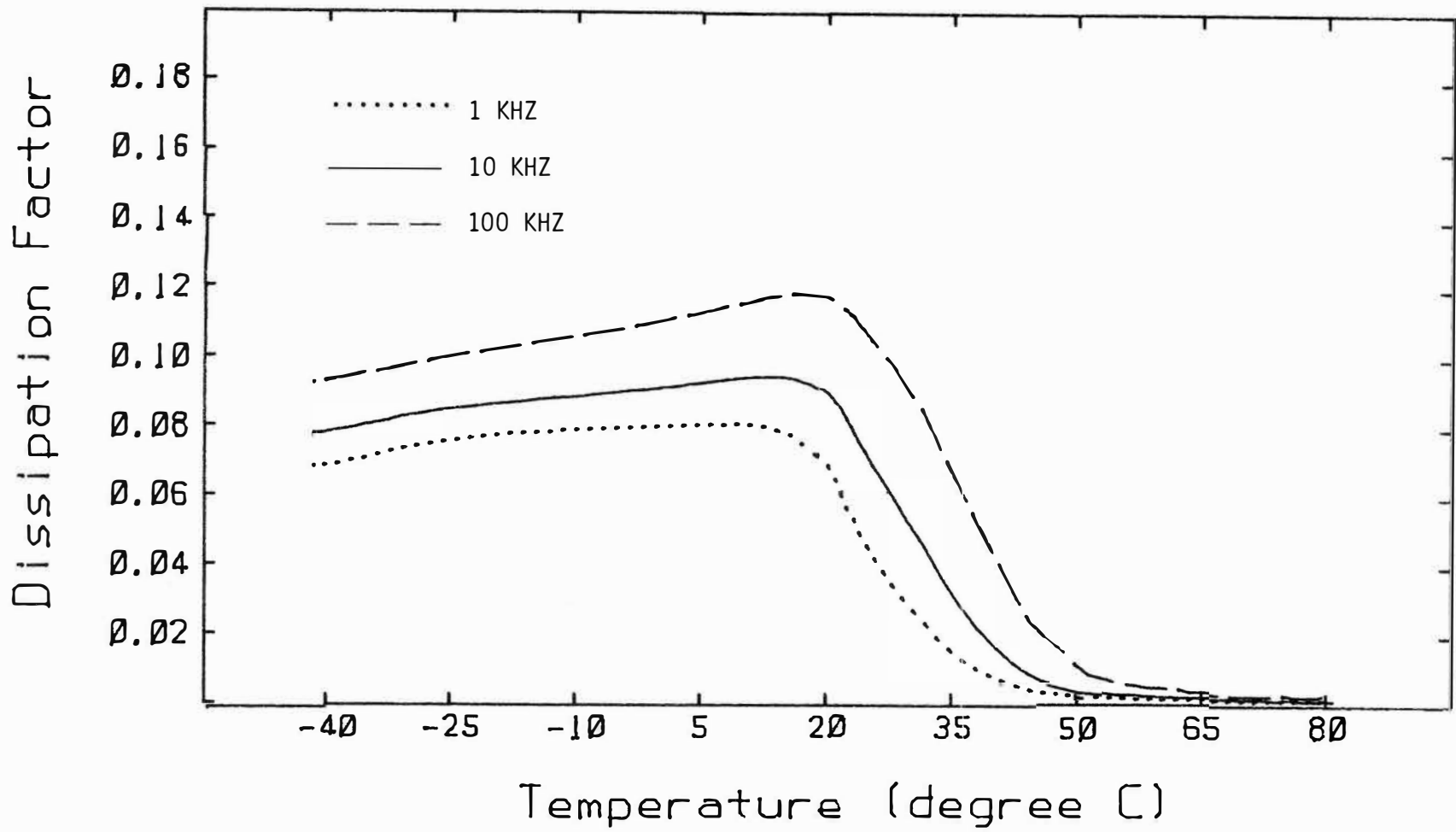


Figure 27. Dissipation Factor vs. Temperature for P₃MN-PT with 3.3 m% Excess PbO Sintered for 3 hours at 1000°C.

point shifts to higher temperatures with increasing frequency. An increase of the maximum dielectric constant with increasing sintering temperature can also be seen in these figures. The dielectric constant, dissipation factor and Curie temperature data of this study are listed in Appendix C.

The dielectric constant and dissipation factor of the capacitors were reported as the average of the optimal values obtained from 2 sets of specimens. As a consequence of the presence of a liquid phase during sintering, PbO was lost from the liquid phase and from the $P_3\text{MN-PT}$ solid solution. It was found that the dielectric properties are related to the sintered density and microstructure.

In general, a dense and second-phase-free dielectric is a prerequisite for optimal dielectric properties. Therefore, the optimal properties should result from specimens sintered such that the weight loss just equals the amount of excess PbO added. The structure of these specimens should both have the highest density and be the most second-phase-free of all the specimens for each composition sintered at a given temperature.

As can be seen in figures 28 and 29 the dielectric constant increases with increasing sintering temperature. Dielectric constant is not directly related to the bulk density, as can be seen by comparing figures 28 and 29 with fig. 8 and 9. The dielectric properties must depend on the microstructures as well. As can be seen from figure 12 and 21,

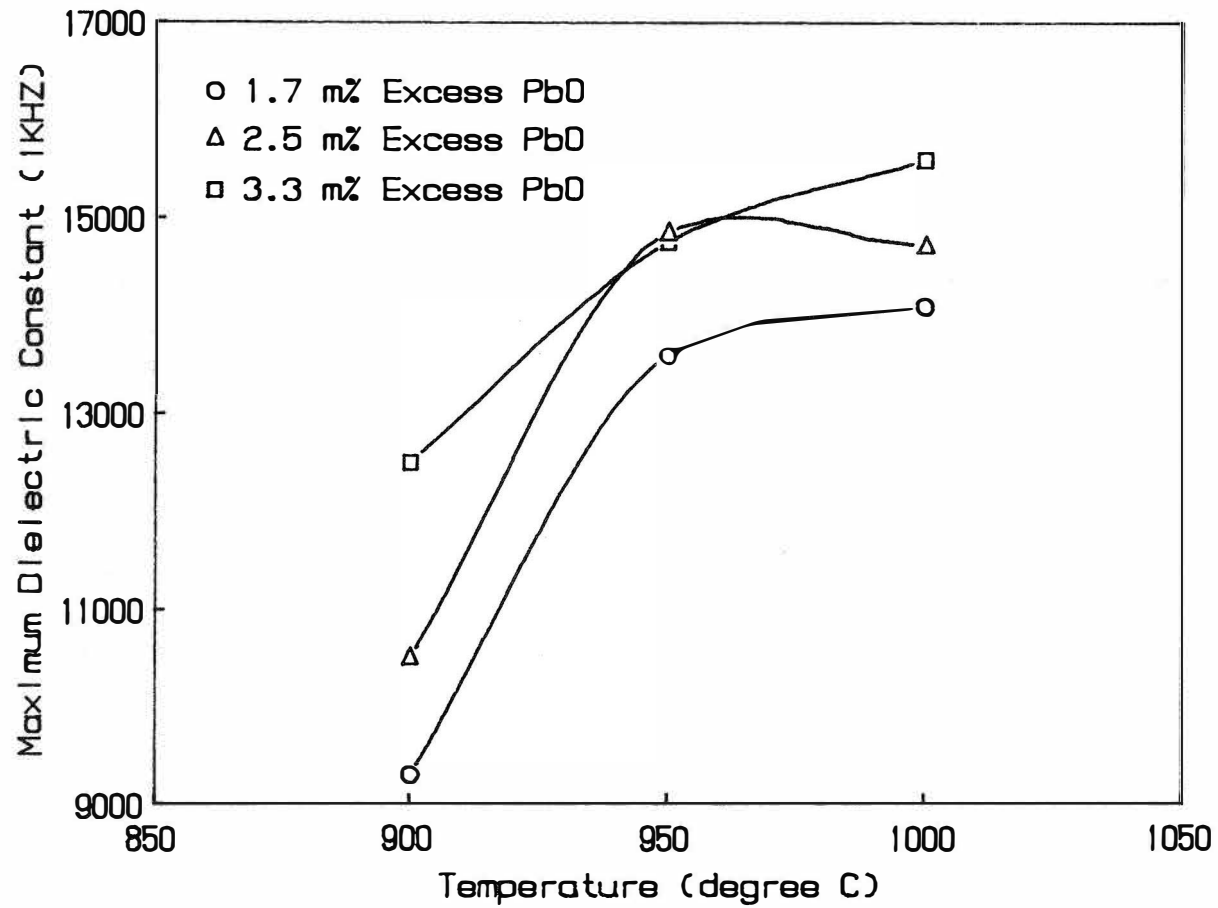


Figure 28. Maximum Dielectric Constant at 1 KHZ vs. Sintering Temperature for P₃MN-PT with Excess PbO Sintered for 3h.

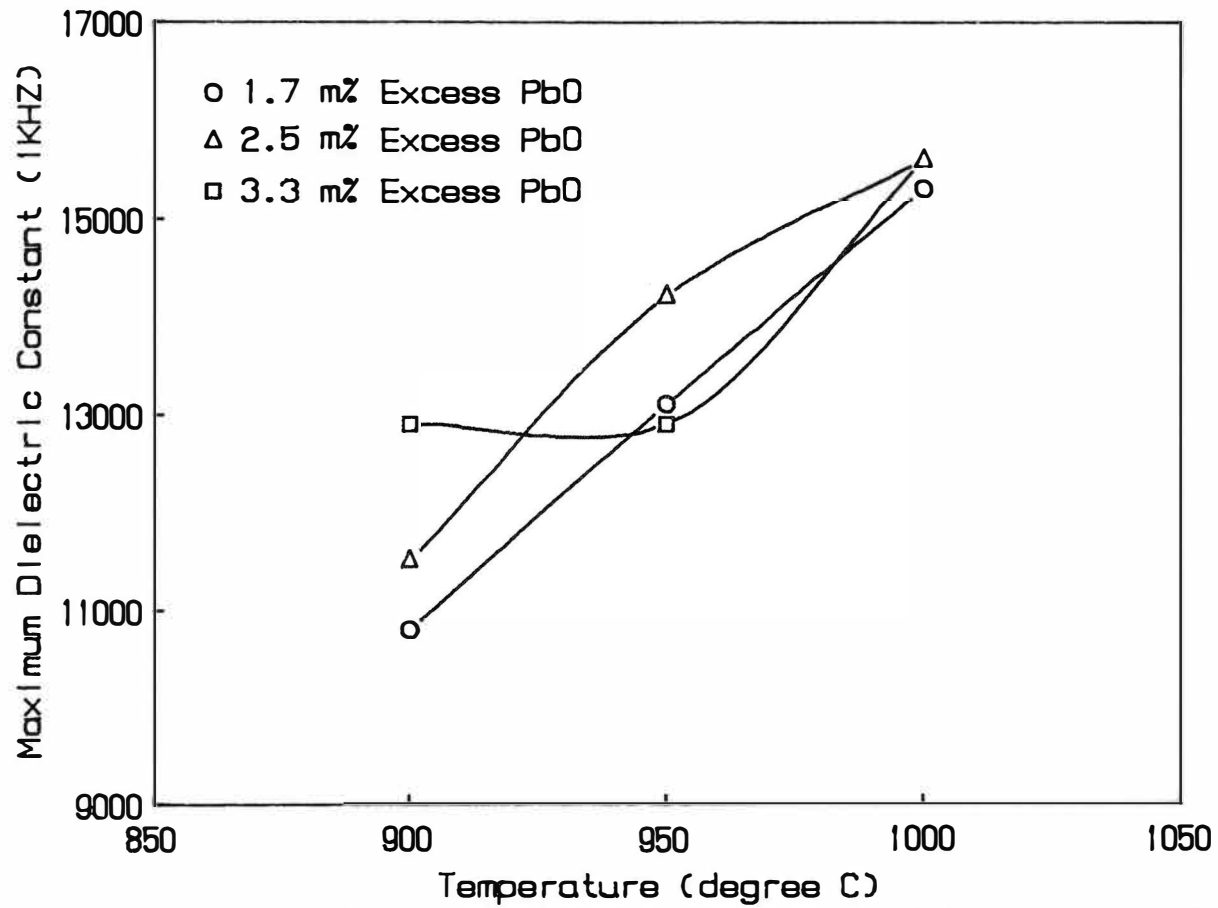


Figure 29. Maximum Dielectric Constant at 1 KHZ vs. Sintering Temperature for P₃MN-PT with Excess PbO Sintered for 5h.

a specimen with 3.3 m% excess PbO sintered at 1000°C for 3h exhibits a higher dielectric constant. It also shows an enhanced grain growth as compared with a specimen with 2.5 m% excess PbO sintered at 950°C for 3h. The fact that the dielectric constant increases with increasing sintering temperature seems to indicate that grain growth may be related to the increase of the dielectric constant.

The resistivities of all the capacitors obtained were on the order of 10^{10} ohm-cm as compared with those obtained at sintering temperatures over 1200°C, which are of the order of 10^{12} ohm-cm.

For the base composition used in this study, the Curie temperature was expected to be at 35°C. As can be seen in Appendix C, the Curie temperature for all of the compositions is 35 ± 5 °C. In general, the Curie temperature decreases with increasing sintering temperature (from 38°C for sintering at 900°C to around 33°C at 1000°C). This might be due to the PbO loss, which decreases the PbO content of the solid solution more severely at higher sintering temperatures.

V. CONCLUSION

1) The reaction between MgNb_2O_6 and PbO at 750°C yielded nearly pure P_3MN phase.

2) The addition of excess PbO to a P_3MN - PT based composition resulted in densities greater than 96 % of theoretical density at temperatures as low as 900°C .

3) The final densities of the specimens with excess PbO sintered in the 900 to 1000°C temperature range depends upon the loss of PbO . Excessive PbO losses deteriorate the densification at 1000°C for sintering times greater than 1 hour.

4) The solid solution P_3MN - PT with 3.3 m% excess PbO , which was sintered at 1000°C for 1 hour, yielded capacitors with a maximum dielectric constant of 17,000 at 1 kHz.

BIBLIOGRAPHY

1. Smolenskii, G.A., and A.I. Agranovskaya, "Dielectric Polarization of a Number of Complex Compounds," Soviet Physics- Solid State, Vol. 2, No. 10, 1959, pp. 1429-1437.
2. Smolenskii, G.A., and A.I. Agranovskaya, "Ferroelectrics with Diffuse Phase Transitions," Soviet Physics- Solid State, Vol. 2, No. 11, 1961, pp.2584-2593.
3. Bokov, V.A., and I.E. Myl'nikova, "Ferroelectric Properties of Monocrystals of New Perovskite Compounds," Soviet Physics- Solid State, Vol. 2, No. 11, 1961, pp. 2428 -2432.
4. Furukawa, K., S., Fujiwara, and T. Ogasawara, "Dielectric Properties of $\text{Pb}(\text{Mg}_{1/3}\text{Nb}_{2/3})\text{O}_3 - \text{PbTiO}_3$ Ceramics for Capacitor Materials," Proceedings of the Japan-U.S. Study Seminar on Dielectric and Piezoelectric Ceramics P.T-4, 1982.
5. Ouchi, H., K.Nagano, and S.Hayakawa, "Piezoelectric Properties of $\text{Pb}(\text{Mg}_{1/3}\text{Nb}_{2/3})\text{O}_3 - \text{PbTiO}_3 - \text{PbZrO}_3$ Solid Solution Ceramics," Journal of the American Ceramic Society, Vol.48, No. 12, 1965, pp.630-635.

BIBLIOGRAPHY (Continued)

6. LeJeune, M., and J.P. Boilot, "Formation Mechanism and Ceramic Process of the Ferroelectric Perovskites: $\text{Pb}(\text{Mg}_{1/3}\text{Nb}_{2/3})\text{O}_3$ and $\text{Pb}(\text{Fe}_{1/2}\text{Nb}_{1/2})\text{O}_3$," Ceramics International, Vol. 8, No. 3, 1982, pp. 99-103.

7. Swartz, S.L., and T.R. Shrout, "Fabrication of Lead Magnesium Niobate," Materials Research Bulletin, Vol. 17, 1982, pp. 1245-1250.

8. Shrout, T.R., and S.L. Swartz, "Dielectric Properties of Pyrochlore Lead Magnesium Niobate," Materials Research Bulletin, Vol. 18, 1983, pp. 663-667.

9. Eisa, M.A., M.F. Abadir, and A.M. Gadalla, "The System TiO_2 -Pb-O in Air," Transaction Journal of the British Ceramic Society, Vol. 79, No. 4, 1980, pp. 100-104.

10. Guha, J.P., and Anderson H.U., "Low Firing Dielectric Ceramics Based on $\text{P}_3\text{MN-PT}$ Solid Solution," Annual Meeting of the American Ceramic Society, May 1986.

BIBLIOGRAPHY (Continued)

11. LeJune, M., and J.P. Boilot, "Optimization of Dielectric Properties of Lead-Magnesium Niobate Ceramics," Ceramic Bulletin, Vol. 65, No. 4, 1986, pp. 679-682.

12. Smolenskii, G.A., and A.I. Agranovskaya, "Dielectric Polorization and Losses of Some Complex Compounds," Soviet Physics- Techical Physics, Vol. 3, 1958, pp.1380-1382.

13. Bokov, V.A., and I.E. Myl'nikova, "Electrical and Optical Properties of Single Crystals of Ferroelectrics with a Diffused Phase Transition," Soviet Physics-Solid State, Vol. 3, No. 3, 1961, pp. 613-623.

14. Smolenskii, G.A., A.I. Agranovskaya, and S.N.Popov, "On the Mechanism of Polarization in Solid Solutions of $Pb_3NiNb_2O_9$ - $Pb_3MgNb_2O_9$," Soviet Physics-Solid State, Vol. 1, No.1, 1959, pp. 147 -148.

15. Fritsberg, V. Ya, and P.A. Fritsberg, "Dielectric Properties of Lead Magnesium Niobate Under High Hydrostatic Pressure Near a Phase Transition Point," Soviet Physics- Crystallography, Vol. 24, No. 4, 1979, pp. 492-493.

BIBLIOGRAPHY (Continued)

16. Setter, N., and L.E. Cross, "An Optical Study of the Ferroelectric Relaxors $\text{Pb}(\text{Mg}_{1/3}\text{Nb}_{2/3})\text{O}_3$, $\text{Pb}(\text{Sc}_{1/2}\text{Ta}_{1/2})\text{O}_3$, and $\text{Pb}(\text{Sc}_{1/2}\text{Nb}_{1/2})\text{O}_3$," Ferroelectrics, Vol. 37, 1981, pp.551-554.

17. Ouchi, H., M. Nishida, and S. Hayakawa, "Piezoelectric Properties of $\text{Pb}(\text{Mg}_{1/2}\text{Nb}_{2/3})\text{O}_3$ - PbTiO_3 - PbZrO_3 Ceramics Modified with Certain Additives," Journal of the American Ceramic Society, Vol. 49, No.11, 1966, pp.577-582.

18. Bonner, W.A., E.F. Dearborn, J.E. Geusic, H.M. Marcos, and L.G. Van Uitert, "Dielectric and Electro-optic Properties of Lead Magnesium Niobate," Applied Physics Letters, Vol. 10, No. 5, 1967, pp. 163-165.

19. Uchino, K., S. Nomura, L.E. Cross, S.J. Jang, and R.E. Newnham, "Electrostrictive Effect in Lead Magnesium Niobate Single Crystals," Journal of Applied Physics, Vol. 51, No. 1, 1980, pp. 1142-1145.

20. Jang, S.J., K. Uchino, S. Normura, and L.E. Cross, "Electrostrictive Behavior of Lead Magnesium Niobate Based Ceramic Dielectrics," Ferroelectrics, Vol. 27, 1980, pp. 31-34.

BIBLIOGRAPHY (Continued)

21. Cross, L.E., S.J. Jang, R.E. Newnhan, S. Nomura, and K. Uchino, "Large Electrostrictive Effects in Relaxor Ferroelectrics," Ferroelectrics, Vol. 23, 1980, pp. 187-192.
22. Nishida, M., S. Kawashima, I. Ueda, and H. Ouchi, "Piezoelectric Ceramics for High Power Use," Journal of the Physics Society of Japan, Vol. 49, 1980, Supplement B, pp. 200-202.
23. LeJune, M., and J.P. Boilot, "Influence of Ceramic Processing on Dielectric Properties of Perovskite Type Compound: $\text{Pb}(\text{Mg}_{1/3}\text{Nb}_{2/3})\text{O}_3$," Ceramics International, Vol. 9, No. 4, pp. 119-122.
24. Swartz, S.L., T.R. Shrout, W.A. Schulze, and L.E. Cross, "Dielectric Properties of Lead-Magnesium Niobate Ceramics," Journal of the American Ceramic Society, Vol. 67, No. 5, 1984, pp. 311-315.
25. Guha, J.P., "Comment on 'Dielectric Properties of Lead-Magnesium Niobate Ceramics'," Communications of the American Ceramic Society, 1985, pp. C-86-C-87.

BIBLIOGRAPHY (Continued)

26. Chu, M.S.H., and C.E. Hodgkins, TAM Ceramics, Inc.,
"High K (15000) Y5U Composition with Ultra Low Firing
Temperature (950°C) for Multilayer Ceramic Capacitors,"
American Ceramic Society 87th Annual Meeting, Cincinnati,
Ohio, 1985.

VITA

Dyllan Jye-Lun Hong was born on August 30, 1961 in Kaushiung, Republic of China. He received his primary and secondary education in Taipei, Taiwan. In June of 1983 he received his Bachelor of Science in Materials Science and Engineering from National Tsing Hua University in Shin-Chu, Taiwan. He joined the R.O.C Army as a Second Lieutenant Training Officer of Artillery in July, 1983 and retired from the Army in May, 1985. In August of 1985 he entered the University of Missouri-Rolla to pursue his Master of Science degree in Ceramic Engineering. He is a member of the American Ceramic Society.

APPENDIX A

CALCULATION FOR THEORETICAL DENSITY

1. Basic Composition:

$$P_3MN \quad : \quad 92 \quad \text{wt\%}$$

$$PT \quad : \quad 8 \quad \text{wt\%}$$

Molar % of P_3MN

$$= 92 / 975.69 \times (92/975.69 + 8/303.09)$$

$$= 78.13 \text{ (mol \%)}$$

Molar % of PT

$$= 8 / 975.69 \times (92/975.69 + 8/303.39)$$

$$= 21.87 \text{ (mol \%)}$$

2. Molecular Weight of Basic Composition

$$= 975.69 \times 78.13\% + 303.09 \times 21.87\%$$

$$= 828.59 \text{ (g/mole)}$$

3. Lattice Constant of Basic Composition

$$= \text{d-spacing of (100) peak in X-ray pattern}$$

$$= 4.056 \text{ (\AA)}$$

4. The Number of Atoms Per Molecule of Basic Composition

$$= 15 \times 78.13\% + 5 \times 21.87\%$$

$$= 12.81 \text{ (atoms/molecule)}$$

APPENDIX A (Continued)

5. The Number of Atoms Per Unit Cell of P_3MN-PT

$$= 1 + 1/2 \times 6 + 1/8 \times 8$$

$$= 5 \text{ (atoms)}$$

Theoretical Density of Basic Composition

$$= 828.59 \times 5 / 12.81 \times 6 \times 10^{23} \times (4.056 \times 10^{-8})^3$$

$$= 8.07 \text{ (g/cm}^3 \text{)}$$

APPENDIX B

SAMPLE BULK DENSITY, SHRINKAGE AND WEIGHT LOSS

SAMPLE	Bulk Density g/cc \pm .02	%TD	Shrinkage % \pm .2	Weight Loss % \pm .05	Apparent Porosity % \pm .05
--------	-----------------------------------	-----	-------------------------	-------------------------------	-------------------------------------

1.7 m% PbO Addition

sintered at

900°C for 3 hrs	7.46	92.4	7.0	0.38	0.33
900°C for 4 hrs	7.59	94.0	7.4	0.42	0.58
900°C for 5 hrs	7.76	96.2	7.6	0.45	1.05
900°C for 6 hrs	7.57	93.8	7.2	0.83	1.10
950°C for 1 hr	7.68	95.2	7.2	0.40	0.75
950°C for 2 hrs	7.70	95.4	7.4	0.54	0.38
950°C for 3 hrs	7.67	95.0	7.2	0.59	0.22
950°C for 4 hrs	7.66	94.9	7.2	0.70	0.58
950°C for 5 hrs	7.65	94.8	7.2	0.79	0.60
1000°C for 1 hr	7.62	94.4	7.8	0.41	0.53
1000°C for 3 hrs	7.62	94.4	7.8	0.84	0.10
1000°C for 5 hrs	7.57	93.8	7.4	1.05	0.10

2.5 m% PbO Addition

sintered at

900°C for 3 hrs	7.50	92.9	8.0	0.50	0.94
900°C for 4 hrs	7.68	95.2	7.8	0.57	0.22

APPENDIX B (Continued)

900°C for 5 hrs	7.64	95.2	8.2	0.62	0.58
900°C for 6 hrs	7.62	94.4	7.4	0.85	0.26
950°C for 1 hr	7.63	94.5	7.4	0.44	0.43
950°C for 2 hrs	7.64	94.7	7.4	0.60	0.30
950°C for 3 hrs	7.68	95.2	7.8	0.64	0.53
950°C for 4 hrs	7.61	94.3	7.2	0.75	0.26
950°C for 5 hrs	7.59	94.0	7.2	0.89	0.16
1000°C for 1 hr	7.59	94.0	7.8	0.62	0.20
1000°C for 3 hrs	7.49	92.8	7.4	0.99	0.05
1000°C for 5 hrs	7.50	92.9	7.6	1.40	0.27

3.3 m% PbO Addition

sintered at

900°C for 3 hrs	7.51	93.1	7.8	0.70	0.76
900°C for 4 hrs	7.67	95.0	8.2	0.76	0.56
900°C for 5 hrs	7.67	95.0	8.2	0.86	1.31
900°C for 6 hrs	7.65	94.8	8.0	1.23	1.15
950°C for 2 hrs	7.56	93.7	7.6	0.70	1.06
950°C for 3 hrs	7.61	94.3	7.8	0.75	0.20
950°C for 4 hrs	7.51	93.1	6.8	0.85	0.22
950°C for 5 hrs	7.51	93.1	6.8	1.08	0.20

APPENDIX B (Continued)

1000°C for 1 hr	7.63	94.5	7.4	0.79	0.93
1000°C for 3 hrs	7.46	92.4	7.4	1.44	1.26
1000°C for 5 hrs	7.43	92.1	7.8	1.62	1.31

APPENDIX C

MAXIMUM DIELECTRIC CONSTANT, CURIE TEMPERATURE
DISSIPATION FACTOR AND RESISTIVITY AT T_c

SAMPLE	T_c ($^{\circ}$ C)	K_{max} at 1 KHZ	D.F. %	Resistivity ohm-cm
1.7 m% PbO Addition				
sintered at				
900 $^{\circ}$ C for 3 hours	39	9300	2.1	2.3×10^9
900 $^{\circ}$ C for 4 hours	38	10500	1.7	2.1×10^9
900 $^{\circ}$ C for 5 hours	40	10800	1.6	2.3×10^9
900 $^{\circ}$ C for 6 hours	36	9600	1.8	1.0×10^9
950 $^{\circ}$ C for 1 hour	35	13800	1.6	2.5×10^9
950 $^{\circ}$ C for 2 hours	35	14500	2.2	4.8×10^{10}
950 $^{\circ}$ C for 3 hours	34	13600	1.5	4.2×10^{10}
950 $^{\circ}$ C for 4 hours	34	13400	1.4	6.0×10^{10}
950 $^{\circ}$ C for 5 hours	34	13200	1.4	6.0×10^{10}
1000 $^{\circ}$ C for 1 hours	33	16000	2.3	6.0×10^{10}
1000 $^{\circ}$ C for 3 hours	34	14000	1.5	1.2×10^{10}
1000 $^{\circ}$ C for 5 hours	34	15300	1.5	1.2×10^{10}
2.5 m% PbO Addition				
sintered at				
900 $^{\circ}$ C for 3 hours	37	10500	1.6	2.4×10^{11}

APPENDIX C (Continued)

900°C for 4 hours	38	11100	1.3	1.4×10^{10}
900°C for 5 hours	39	11500	1.6	6.0×10^{11}
900°C for 6 hours	37	10800	2.2	6.0×10^{10}
950°C for 1 hour	34	12300	1.6	5.0×10^{10}
950°C for 2 hours	35	13000	1.7	4.8×10^{10}
950°C for 3 hours	35	14900	1.7	1.0×10^{10}
950°C for 4 hours	34	14400	2.3	4.8×10^{10}
950°C for 5 hours	35	14200	2.2	6.8×10^9
1000°C for 1 hours	34	15200	1.2	3.0×10^{11}
1000°C for 3 hours	33	14700	2.2	1.5×10^{10}
1000°C for 5 hours	35	15600	1.3	1.2×10^{11}
3.3 m% PbO Addition				
sintered at				
900°C for 3 hours	34	12500	1.2	1.2×10^{11}
900°C for 4 hours	38	12700	1.9	3.2×10^{10}
900°C for 5 hours	38	12900	2.4	2.0×10^9
900°C for 6 hours	41	12600	3.1	2.5×10^9
950°C for 2 hours	34	12600	1.3	5.8×10^{10}
950°C for 3 hours	35	14600	1.2	1.2×10^{11}
950°C for 4 hours	35	13400	1.5	6.6×10^{10}
950°C for 5 hours	34	12900	1.2	8.8×10^{10}